Journal of Structural Geology 33 (2011) 500–518

Contents lists available at ScienceDirect

Journal of Structural Geology

journal homepage: www.elsevier.com/locate/jsg

# EBSD microfabric study of pre-Cambrian deformations recorded in quartz pebbles from the Sierra de la Demanda (N Spain)

B. Ábalos [a,*], P. Puelles [a], S. Fernández-Armas [b], F. Sarrionandia [a]

[a] Departamento de Geodinámica, Universidad del País Vasco, PO Box 644, E-48080 Bilbao, Spain
[b] Servicios Generales de Investigación-SGIKER, Universidad del País Vasco, PO Box 644, E-48080 Bilbao, Spain

ARTICLE INFO

*Article history:*
Received 29 July 2010
Received in revised form
28 December 2010
Accepted 8 January 2011
Available online 19 January 2011

*Keywords:*
Quartz
Petrofabric
EBSD
Proterozoic
Cambrian
Iberian Ranges
Spain

ABSTRACT

We describe a new method for the reorientation of lattice preferred orientation data in the absence of a pre-constrained kinematic reference frame. The method enables us to present conventional quartz fabric diagrams after measurements taken from rock sections with a general orientation with respect to foliation and lineation. A microstructural and Electron Back-Scattered Diffraction (EBSD) study of quartz pebbles in early Cambrian conglomerates following this method permit us to recognize a variety of fabrics that resulted from syn-metamorphic ductile deformation under variable temperatures up to 650 °C. The likely source area of the conglomerates was a Proterozoic basement. Candidates for source rock correlations include Neoproterozoic units similar to those outcropping in the northern Iberian Massif, Neoproterozoic medium- to high-grade metamorphic rocks as those outcropping in SW Iberia, or a Neoarchean to Mesoproterozoic concealed basement.



## 1. Introduction

The relationships between sedimentary Cambrian successions and older rock units have traditionally been a matter of active research in the geological literature (Van Hise and Leith, 1909). This has been also the case for the Iberian Peninsula (Vidal et al., 1994), where the analysis has often been hampered by the paucity of relevant "Rosetta-stone" (Hatcher, 1995) outcrops. Conglomerate pebbles from unconformable formations often carry a memory of the precedent tectono-sedimentary history, encapsulated in structures and microfabrics that originally were formed in their source rocks. Structural analysis of such pebble fabrics is usually precluded by the difficulty, or impossibility, to unravel a clear external structural reference framework to which refer any petrographic observation or petrofabric measurement following the conventional procedures (Passchier and Trouw, 1996). Rock fabrics are related to second-rank tensorial physical quantities and thus are intrinsic attributes independent of the external reference system. A corollary to this is that the perspective of microstructures and three-dimensional crystallographic orientations provided by any two-dimensional section of a rock is thoroughly constrained by its petrofabric. Accordingly, the former might also be used to unravel the latter and show it in the conventional fabric representations, provided that pertinent spatial rotations are accomplished.

Outcrops of unconformable Cambrian sediments in contact with Proterozoic rocks in the northwestern Iberian Massif show that an angular unconformity separates them and that the latter were regionally deformed, locally intruded by igneous suites, and mildly metamorphosed before the Cambrian (de Sitter, 1961; Julivert and Martínez García, 1967; Matte, 1967; Marcos, 1973; Pérez Estaún, 1973; Martínez Catalán, 1985; Díaz García, 2006). In correlatable outcrops of the central Iberian Ranges (Colchen, 1974; Álvaro and Vennin, 1998; Liñán et al., 2002) various authors also unravelled the unconformable relationships between the Cambrian and the Neoproterozoic (Schmidt-Thomé, 1973; Liñán and Tejero, 1988). Ábalos (2001) and Álvaro et al. (2008) reported microstructural and metamorphic features postdated by the lowermost Cambrian rocks that permit recognition of the Cadomian orogeny (late Neoproterozoic to early Cambrian) in the area.

It is thought that magmatic arcs and back-arc basins are the Cadomian tectonic settings preserved in the Iberian Peninsula (Ugidos et al., 1997; Fernández Suárez et al., 1998). The Proterozoic basement source for the Neoproterozoic sedimentary basin does not outcrop and very little is known on its lithological nature (Vidal et al., 1994). Ugidos et al. (2010) reported a remarkable geochemical homogeneity in the Upper Neoproterozoic series of central and

* Corresponding author. Tel.: +34 4 6012628; fax: +34 4 6013500.
*E-mail address:* benito.abalos@ehu.es (B. Ábalos).

0191-8141/$ – see front matter © 2011 Elsevier Ltd. All rights reserved.
doi:10.1016/j.jsg.2011.01.005

northwestern Spain, likely suggesting an extensive and homogenized source region. Other Proterozoic constituents of Iberia include granulite-facies allochthonous blocks (interpreted as lower crustal fragments) recovered from deep submarine exploration in the thinned continental margins of the Bay of Biscay and in the Galicia Bank (Gardien et al., 2000). The earliest Cambrian successions cropping out in the core of the Asturian arc and in the Iberian Ranges contain conglomerate layers that might preserve relics of such a concealed basement.

In this article we describe a new method for the reorientation of lattice preferred orientation data in the absence of a pre-constrained kinematic reference frame. The method enables us to present conventional quartz fabric diagrams measured in rock sections with a general orientation with respect to foliation and lineation. We apply the technique to investigate the fabric of ductilely deformed quartz pebbles contained by an early Cambrian conglomerate of North Spain and discuss its implications in the Proterozoic geology of the Iberian Peninsula.

## 2. Geological context

### 2.1. Regional geology

The "Sierra de la Demanda" of N Spain forms the northwestern extension of the Iberian Ranges (Fig. 1). This massif contains thick Cambro-Ordovician successions correlated with coeval and

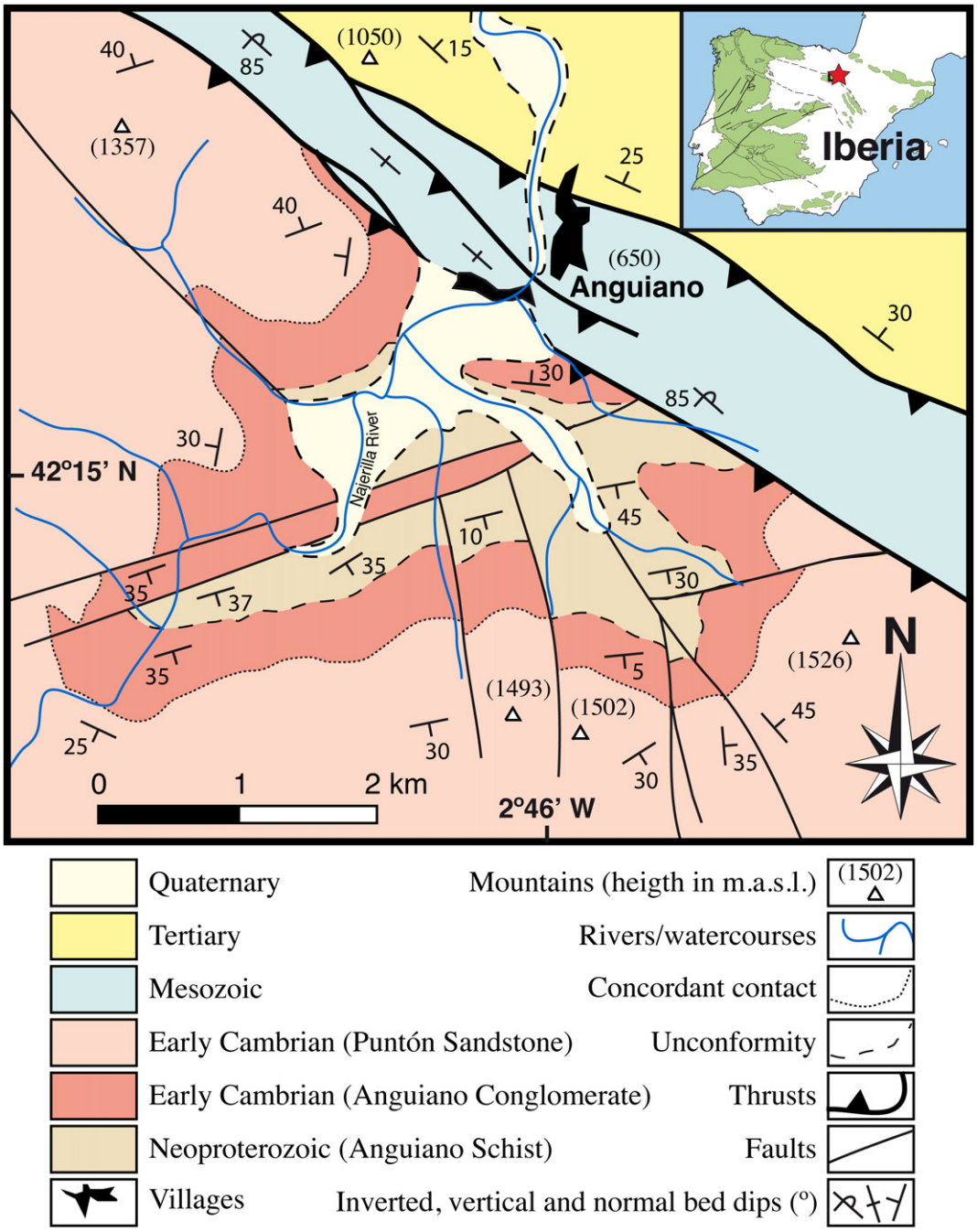


**Fig. 1.** Geological sketch map (after Ramírez Merino et al., 1990) of the area to the South of Anguiano and (inset) regional geological context of the Sierra de la Demanda massif. Inset shows pre-Mesozoic outcrop distribution in the Iberian Peninsula.

sedimentologically similar series of the West-Asturian-Leonese Zone of the Iberian Massif (Carls, 1983; Gozalo and Liñán, 1988). The early Paleozoic rocks were deformed and mildly metamorphosed during the Variscan orogeny (Colchen, 1974) and were unconformably overlain by unmetamorphosed Triassic siliciclastics of the germano-type "Buntsandstein" facies, as well as by younger successions. Tertiary ("Alpine") inversion tectonism is manifested in the area by N-verging major thrusts and associated folds, as well as by variably intense ductile strain (Liesa and Casas Sainz, 1994; Gil Imaz, 2001; Capote et al., 2002).

The occurrence of Cambrian rocks that overlie azoic sediments in the "Sierra de la Demanda" (N Spain) was first realized by Schriel (1930) and afterwards by Lotze (1961). Colchen (1974) disclosed the stratigraphic organization of these rocks, which was refined by Palacios (1982) and Shergold et al. (1983). The largest outcrops of Early Cambrian rocks occur in the eastern part of the Sierra de la Demanda, to the South of Anguiano (La Rioja), dissected by the Najerilla River (Fig. 1). These are pre-trilobitic siliciclastic successions containing a basal (up to 300 m thick) unfoliated quartz-rich conglomerate formation ("Anguiano Conglomerate") overlain by sandstones and quartzites ("Areniscas del Puntón"). The lowermost conglomerate beds are stratigraphically 600 m below the oldest trilobite-bearing Cambrian beds (Palacios, 1982; Palacios and Vidal, 1992; Liñán et al., 1993, 2002).

Neoproterozoic slates ("Anguiano Schists"; cf. Lotze, 1957; Colchen, 1974) crop out under the "Anguiano Conglomerate" (Fig. 1). These are azoic, dark siltstones and mudstones with interbedded sandstone layers. This unit has a maximum thickness of 100–150 m, estimated from surface geology (Ramírez Merino et al., 1990). A Neoproterozoic age is attributed to this succession

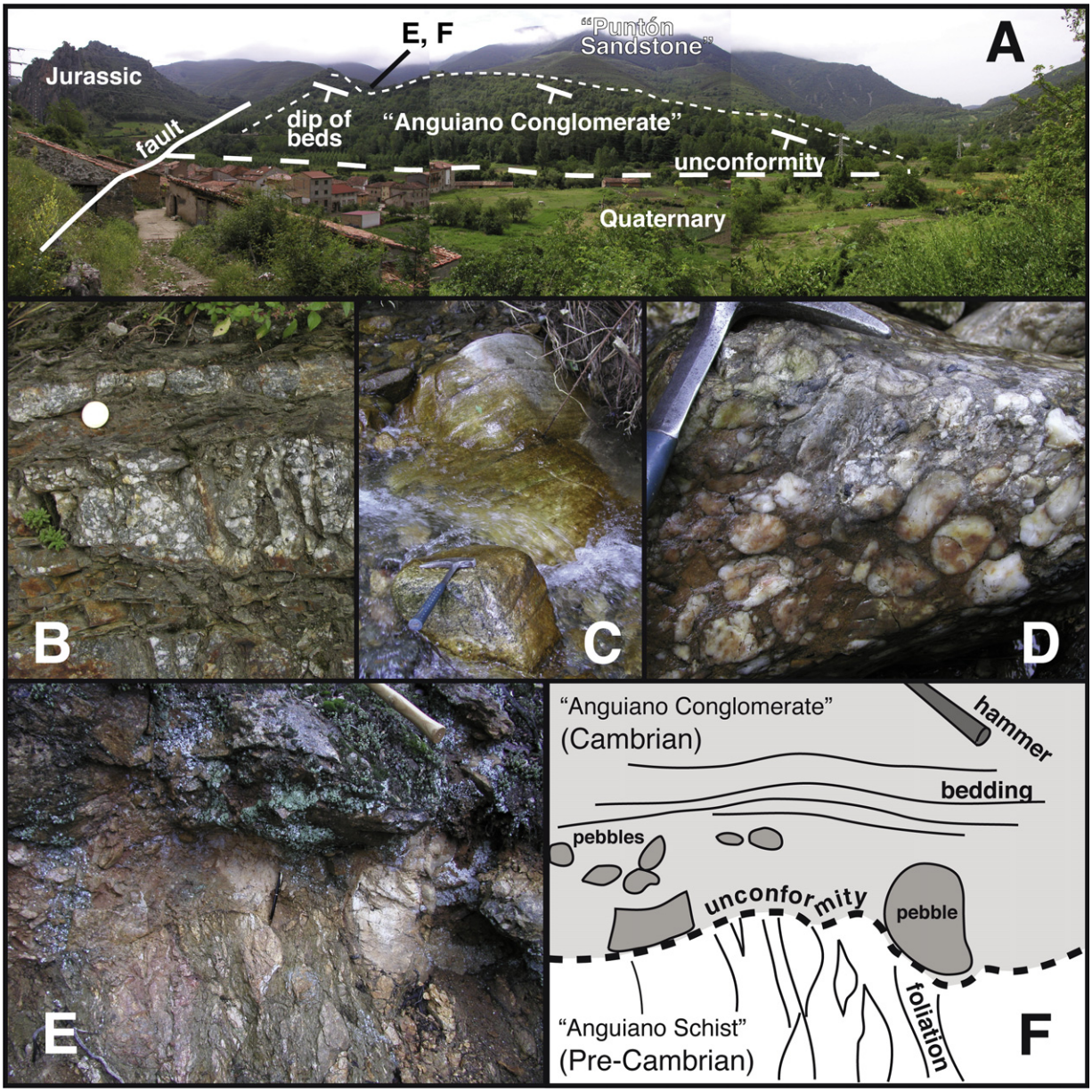


**Fig. 2.** A: View of the Najerilla River Valley near Anguiano (looking toward the South) showing the geological units cited in the text. B: Conglomerate layers interbedded with sandstones in the upper part of the "Anguiano Conglomerate". C: Thick conglomerate beds from the lower part of the "Anguiano Conglomerate". D: Close view of a conglomerate bed with cm-sized, rounded quartzose pebbles. E, F: Field photograph (E) and sketch (F) showing the unconformity between gently (early Cambrian "Anguiano Conglomerate") and steeply dipping (pre-Cambrian "Anguiano Schist") formations. Site location is shown in A.

based upon regional correlations with similar units cropping out about 120 km to the SE ("Paracuellos Group"; Liñán and Tejero, 1988; Valladares et al., 2002a). Gently dipping bedding planes are variably overprinted by a steep foliation associated to subhorizontal intersection lineations and crenulation microfold axes (Ábalos, 2001).

### 2.2. The "Anguiano Conglomerate"

This is an up to 300 m thick siliciclastic succession made of minor sandstone intercalations and of conglomerates (Figs. 1 and 2) with more than 90% of vein quartz, chert or quartzite pebbles (a "quartz-pebble conglomerate" after Cox et al., 2002). The sedimentary structures and the internal organization in sequences suggest a conglomeratic beach sedimentary environment. Bed dips are moderate and no penetrative foliations are observed (Fig. 2A–D). Lotze (1961) suggested that the contact between Cambrian and pre-Cambrian successions is unconformable, whereas Colchen (1974) interpreted that it appears always tectonized. The basal, unconformable contact of the conglomerate is shown in the Fig. 2E–F.

This unit contains abundant, well-rounded silicic pebbles mm to cm in grainsize cemented by diagenetic quartz (e.g.: Figs. 2D and 3A–D). They correspond to five main groups: (I; Fig. 3A) metamorphic polycrystalline quartz aggregates, (II; Fig. 3B) monocrystalline quartz, (III; Fig. 3E) black cherts, (IV) zircon and tourmaline-bearing sandstones and (V; Fig. 3F) foliated quartzites. The undeformed matrix is made of much smaller (diagenetically overgrown) monocrystalline quartz grains (Fig. 3C) and primary porosity was diagenetically filled with quartzose precipitates (Fig. 3D). The matrix includes minor amounts of accessory zircon, tourmaline, rutile and mica. Pressure-solution microstructures can be observed locally. They are shown by small pebbles with ellipsoidal contours partly truncated by the straighter traces of polycrystalline quartz aggregates (Fig. 3A) or by matrix quartz grains that bulge into and dissolve larger monocrystalline quartz pebbles (Fig. 3B). They are also observable as matrix quartz grain syntaxial overgrowths preserving "ghost" inclusions that delineate the rounded shape of the original detrital grains (Fig. 3C). Likely, these microstructures formed early during the diagenesis. Cementation conferred the conglomerates their massive constitution and mechanically competent nature, preserving them from any subsequent strain or foliation development.

Black chert pebbles (Fig. 3E–F) exhibit microstructural evidence of brittle deformation (microfaults, brecciations and thin veins filled by syntaxial fibrous quartz) and are less rounded than other pebbles. They can exhibit ductile deformations, too (microfolds with thickened hinges and axial planar continuous foliations; Fig. 3E). Liñán and Tejero (1988) defined a 4 m thick laminated chert unit with lenticular shales (Fresno Formation) in the Neoproterozoic outcrops of the central Iberian Ranges. However, no evidence of tectonic deformation of this unit prior to deposition of Cambrian successions has been reported. Quartzite and sandstone pebbles often show continuous foliations (Fig. 3F). Sandstone pebbles are made of quartz and less abundant feldspar grains embedded by a finer grained matrix with oriented mica and chlorite. These pebbles often contain detrital tourmaline, rutile and zircon grains (Fig. 3G–H).

Mono- and poly-crystalline quartz pebbles exhibit a variety of microstructures that resulted from dynamic recrystallization, a thermally activated process contemporaneous with deformation in the dislocation creep regime. The concomitant, syn-metamorphic ductile deformations include continuous foliations, quartz grain shape fabrics, various types of subgrain or recrystallized new grain microstructures, and lattice preferred orientations (LPOs). They are described in further detail in the following sections.

## 3. Methods

### 3.1. Current understanding of quartz LPOs

Quartz microstructures and fabrics resulting from ductile deformation are well known in ductilely deformed quartz-tectonites. The deformation regime and active intracrystalline slip systems constrain fabric internal and external symmetry (Bouchez et al., 1983; Price, 1985; Schmid and Casey, 1986; Passchier and Trouw, 1996, and references therein). The interpretations derived from microstructural and fabric studies relate systematically to "oriented" thin sections cut along directions normal to the macroscopic foliation (the XY structural plane) that contain the lineation (the X structural direction). In the Fig. 4 the basic geometrical relationships between the XYZ reference framework and quartz [c] and ⟨a⟩ crystallographic axis orientations are shown schematically for non-coaxial deformations under increasing temperatures, represented in the conventional XZ section of stereographic diagrams.

In the Fig. 5 we summarize the geometrical [c] and ⟨a⟩ crystallographic axis organizations that result from non-coaxial ductile deformation of quartz under temperatures characteristic of low- to medium-grade metamorphism (Fig. 5A–C) and under high-grade metamorphism (Fig. 5D–F). In both situations quartz fabrics permit to identify two perpendicular girdles that contain axis submaxima at specific locations (Fig. 5A and D). As regards the [c] axes, submaxima can occur along the Y structural direction as well as near Z or X, whereas three ⟨a⟩ axis submaxima separated 120° occur either parallel to the plane normal to the foliation (Fig. 5A–B) or along a plane normal to both the [c] axis girdle and to the XZ plane (Fig. 5D–E). The ⟨a⟩ axis maxima are often of different intensity. Depending upon the temperature of deformation, the most intense submaxima can be located close to X (Fig. 5A–B) or to Z (Fig. 5D–E). Under non-coaxial deformations, the [c] axis girdles are oblique to the XYZ reference frame, the angle of this fabric obliquity being constrained by the intensity of non-coaxial deformation and by the relative contribution of coaxial components (subsimple shear; cf. Means et al., 1980).

### 3.2. Analytical methods

Preparation of oriented thin sections directly from quartz pebbles is not possible in the Anguiano Conglomerate since they are mechanically coupled to the matrix and no viable chemical or mechanical separation method is devised. Pebble sections used for the fabric study have, thus, a priori unknown relationships with respect to the conventional XYZ structural framework. Only the foliation trace can be recognized.

Quartz microstructures and fabrics were studied in standard, 30 μm thick polished rock sections. Preliminary studies were performed with a polarizing microscope and a five-axis Leitz universal stage (U-stage). An Electron Back-Scattered Diffraction (EBSD) study was performed on selected thin sections. In order to remove the mechanically damaged uppermost layer, these were ultra-polished using a colloidal silica suspension for 3–5 h. Samples were covered with an Au-Pa layer before polishing completion and finally carbon coated to prevent charging.

Crystallographic orientation measurements were performed at the University of the Basque Country (Faculty of Science and Technology) with an automated electron back-scattered diffraction system (Channel5, HKL) attached to a JEOL JSM-7000F Field Emission Scanning Electronic Microscope (FE-SEM). Samples were

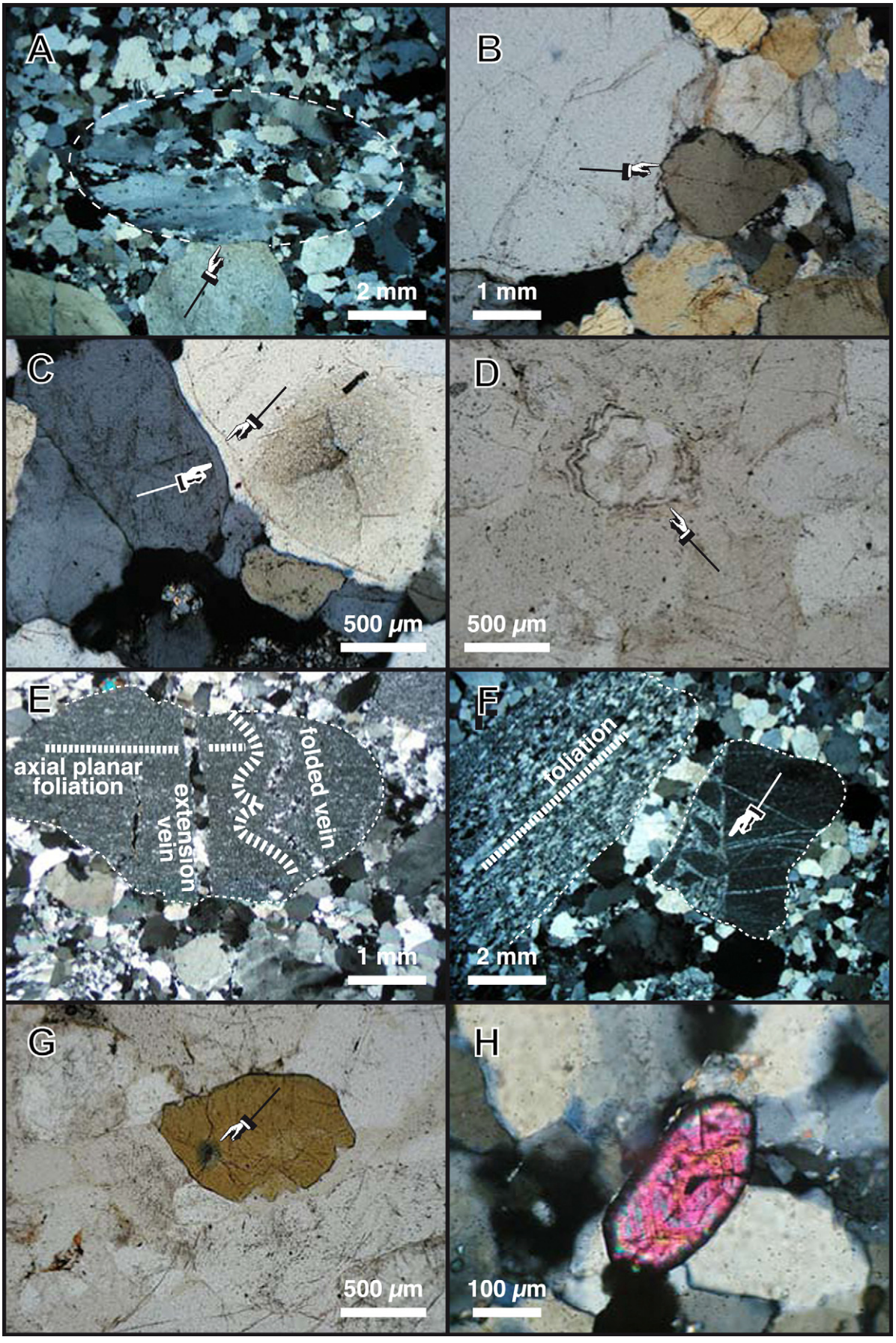
A
2 mm
B
1 mm
C
500 μm
D
500 μm
E
axial planar foliation
extension vein
folded vein
1 mm
F
foliation
2 mm
G
500 μm
H
100 μm

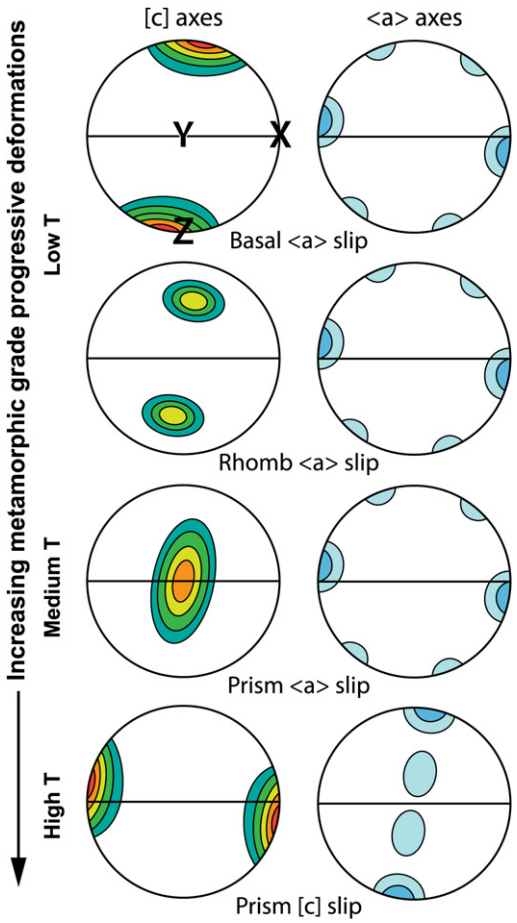


**Fig. 4.** Idealized lower hemisphere stereographic projections showing the relationships between quartz [c] and ⟨a⟩ crystallographic axis fabrics and intracrystalline slip systems operating under increasing temperatures and non-coaxial deformation (after Schmid and Casey, 1986).

mounted in this apparatus on a stage tilted 70°, with the thin section long axis parallel to the FE-SEM X-axis. The beam working distance was 20 mm (Prior et al., 1999). An acceleration voltage of 25 kV, a beam current of ca. 14 nA and a copper tape attached to the sample surface surrounding the measurement area were used to reduce charging effects. Crystallographic orientation solutions with Mean Angular Deviation (MAD) values over 1.2 (between detected and simulated patterns) were rejected to assure EBSD measurement reliability.

Orientation maps and lattice preferred orientation (LPO) pole figures were drawn using the Channel5 software package after automated EBSD analysis on predefined sampling grid steps of 10 μm. These steps are sometimes significantly smaller than the average grainsize of the quartz aggregates and can create artifacts in the pole figure contours. In order to avoid this, we used the software package to isolate the areas of the thin sections occupied by quartz pebbles and, then, to perform automated recognition of subgrains and new grains (Trimby et al., 1998). The crystallographic orientation data were thus filtered so that the actual fabric diagrams of any selected pebble contain one orientation for each grain. To this end, a critical misorientation threshold of 10° was considered (allowing boundary completion down to 5°). Fabric diagrams are presented in lower hemisphere, equal area stereographic projections where the projection planes lack any conventional geometric relationship with respect to the structural XYZ framework of the pebbles. The Orientation Distribution Function (ODF) was calculated from individual orientations with specific Channel5 software packages using a Gaussian bell curve smoothing width of 20°. The strength of the texture was expressed by the texture index *J*, calculated as the mean square value of the ODF.

### 3.3. Fabric rotation procedures

In order to present our fabric study in conventional stereographic diagrams (lower hemisphere projections where the foliation appears vertical oriented E-W and the lineation is horizontal E-W), we envisaged two rotation procedures: one to be applied to U-stage measurements and the second for the EBSD data. In the first case the procedure is based upon the statistical geometric relationships between the orientation of grain boundaries and the XZ structural plane. In the second case the procedure takes into account the geometrical relationships that exhibit quartz [c] (also [0001]) and ⟨a⟩ axes (these including the [11-20] and [10-10] directions) with respect to foliation and lineation (Figs. 4 and 5). Quartz [c] axis can be notated as [0001] or, alternatively (this is the standard notation used by the Channel5 and HKL software), as the pole to the family of planes {0001}, whereas the ⟨a⟩ axes can also be notated as poles to the sets of m-planes {11-20} or {10-10}.

#### 3.3.1. Rotation of U-stage data

As determination of quartz ⟨a⟩ axis orientations with a U-stage is not possible, finding the rotation axes and angles needed to fabric restoration to the conventional microtectonic XZ framework is precluded unless various prerequisites are met. We accomplished U-stage fabric rotations with two pebbles whose quartz microstructure resembled closely well-known examples from the literature. This implied that, whilst a priori the orientation of the XYZ reference frame was general with respect to the edges and plane of the thin sections, likely the X and Z axes were close to be contained in the plane of the pebble thin section, in which the foliation was clearly observable, too. The rotations performed were sequential and included first a vertical axis rotation in order to place the foliation EW in the stereoplots. Then rotations on horizontal E-W and N-S axes enabled us to relocate the foliation vertical E-W with X horizontal. Determination of the vertical axis rotation angle is straightforward from visual inspection of the angle between the pebble foliation and the U-stage E-W referential. The tilt angle needed to reorientate the foliation (XY) perpendicular to the horizontal U-stage plane was determined from the statistical mean of the angles formed between the plane of the thin section and several tens of quartz subgrain boundaries (parallel to prism planes) oriented parallel to the foliation. In a conventional XZ section of a rock specimen this set of grain boundaries is expected

**Fig. 3.** Micrographs showing textural features of the "Anguiano Conglomerate". A: Polycrystalline quartz aggregate pebble showing an internal foliation absent in the surrounding matrix and a pressure-solution contact (marked by the arrow) against a monocrystalline quartz pebble whose original, curved outline appears truncated. B: Small matrix quartz grains bulging into and dissolving (arrow) a larger monocrystalline quartz pebble. C: Diagenetic quartz overgrowths of two monocrystalline quartz grains whose original rounded outlines are still depicted by "ghost" inclusions (marked by the arrows). D: Quartzose diagenetic precipitates with rhythmic and idiomorphic arrangement filling the primary porosity. E: Black chert pebble showing microfolds, an axial planar continuous foliation and an extensional vein normal to it. F: Ellipsoidal quartzite pebble (left) with an internal foliation adjacent to an irregular black chert pebble (right) containing thin quartz-filled cracks and microbreccia. G: Detrital matrix tourmaline grain containing a zircon inclusion that has developed a radioactive damage halo. H: Detrital matrix zircon grain with a slightly rounded contour and internal idiomorphic crystal faces denoting magmatic growth textures. Plane polarized light in D and H and crossed polars in the other micrographs.

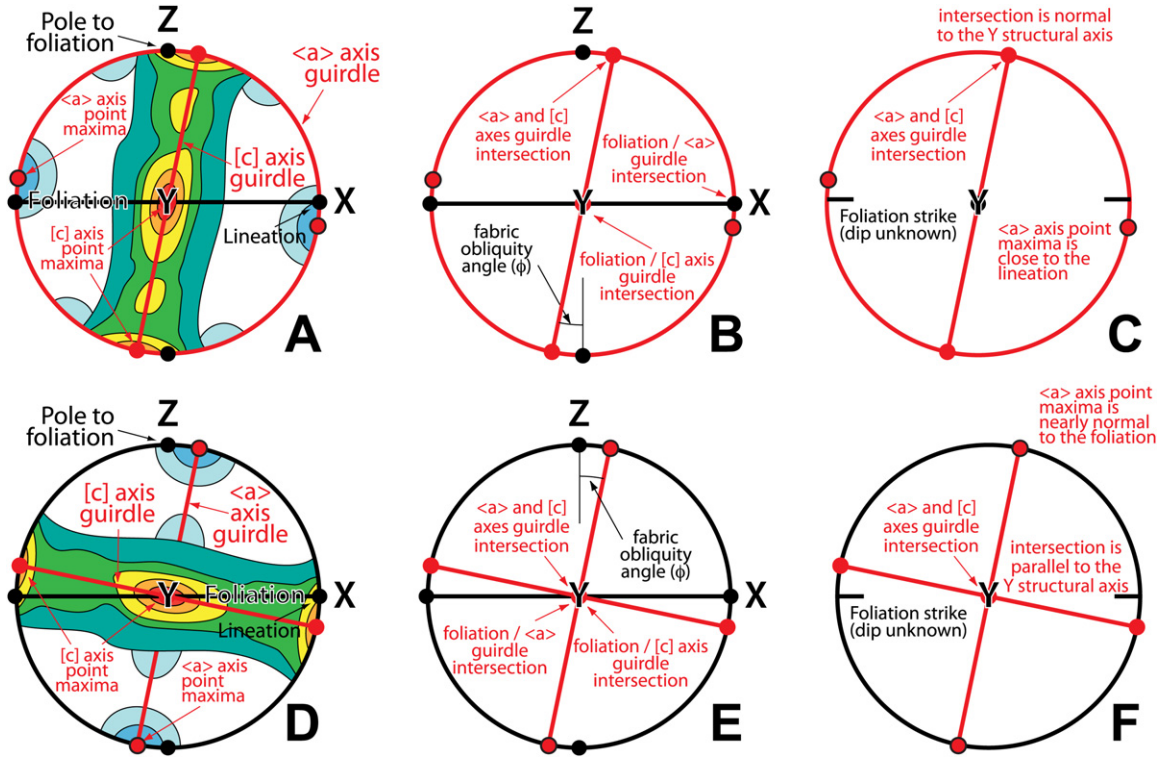


**Fig. 5.** A: Conventional quartz [c] and ⟨a⟩ axis LPOs (equal area, lower hemisphere) resulting from non-coaxial ductile deformation under low- to medium-grade metamorphic temperatures. B: Geometrical relationships between girdle and point maxima intersections with respect to the structural XYZ referential. C: The foliation strike, the principal quartz ⟨a⟩ axis point maxima and the [c]-girdle/⟨a⟩-girdle intersection can be determined directly from LPOs, independent of the internal or external reference framework considered. D: Conventional quartz [c] and ⟨a⟩ axis LPOs resulting from non-coaxial ductile deformation under high-grade metamorphic temperatures. E: Idem as B. F: Idem as C. See text for further details.

to be statistically perpendicular to the plane of the section as well as parallel to the foliation. Similarly, the tilt angle needed to reorientate the X structural direction to a horizontal E-W position was determined with the U-stage from the statistical mean of the angles formed between the plane of the thin section and several tens of subgrain boundaries oriented normal to the foliation.

### 3.3.2. Rotation of EBSD data

In this case the foliation strike (observable in pebble sections) and the ⟨a⟩ and [c] girdles recognizble in EBSD fabric diagrams permitted to constrain the orientation of the XY plane. As depicted by the Fig. 5B–C and E–F, the foliation and the [c] crystallographic axis girdles always intersect parallel to the Y structural direction. Such intersection can be marked directly (Fig. 5D–E; the intersection coincides with Y) or indirectly (Fig. 5A–B; the intersection occurs at 90° to Y) by the ⟨a⟩ and [c] girdles. Once this is achieved, the determination of the Z and X directions is straightforward (Z is normal to the XY plane and X is normal to Y and Z within XY; Fig. 5B and E).

The next step corresponds to rotation of both the crystallographic fabrics measured and their XYZ reference axes to the conventional microtectonic stereographic framework, that consists of a vertical XY plane with X horizontal E-W. Since the EBSD fabric analysis provides complete crystallographic orientation data for quartz ⟨a⟩ and [c] axis girdles and the Channel5 software package requires Euler angles to handle rotations, we actually followed with the EBSD data the procedure described in the Fig. 6. The quartz EBSD fabrics obtained for each pebble sliced with a general orientation permitted to determine ⟨a⟩ and [c] axes best-fit great circles after the stereographic projections. These intersect at a point easy to find (Fig. 6A), as well as is the strike of the foliation (straightforward from inspection of the microstructure).

In low- to moderate-temperature quartz deformation (Fig. 5A–C) the ⟨a⟩ and [c] axes girdle intersection is at 90° from the Y structural axis, which is also contained by the [c] axis girdle (Fig. 6B). The foliation strike and the orientation of Y are then used to establish the orientation of the XY plane and its pole (Fig. 6C). The pole to XY is the Z structural direction (Fig. 6D), which forms an angle (φ, the fabric obliquity angle) with the ⟨a⟩ and [c] girdle intersection when plastic deformation includes rotational components.

In a similar way, in high-temperature quartz deformation (Fig. 5D–F) the ⟨a⟩ and [c] axes girdles intersect along Y. The foliation strike and the orientation of Y can be used to define the orientation of the XY plane, its pole (the Z structural direction) and the X direction (at 90° of Y within XY). Z forms the φ fabric obliquity angle with the pole to the [c] girdle and 90−φ with the pole to the ⟨a⟩ girdle.

Determination of the three Euler angles (α, β and γ) needed to perform rotations requires consideration of orientation of the current X, Y and Z structural axes together with the final position of these reference axes used in conventional fabric stereoplots (Bunge, 1985, pp. 79–80): horizontal E-W (X), N-S (Z) and vertical (Y). The stereoplots drawn by the Channel5 software after raw data use as reference axes three directions: the horizontal E-W ($H(EW)_{EBSD}$ in the Fig. 6E), the horizontal N-S ($H(NS)_{EBSD}$ in the Fig. 6E) and the vertical ($V_{EBSD}$ in the Fig. 6E) which relate to the edges of the rectangular rock thin sections used for measurements. These EBSD reference axes and the crystallographic axes must be sequentially rotated using the Euler angles so that the actual stereoplots can be interpreted conventionally. Determination of the Euler angles α, β and γ requires to locate first the "line of nodes" (Fig. 6E), which is parallel to the intersection between the XZ structural plane and the plane containing the horizontal axes of the EBSD referential. On this basis, α is the angle between the line of nodes and the X structural

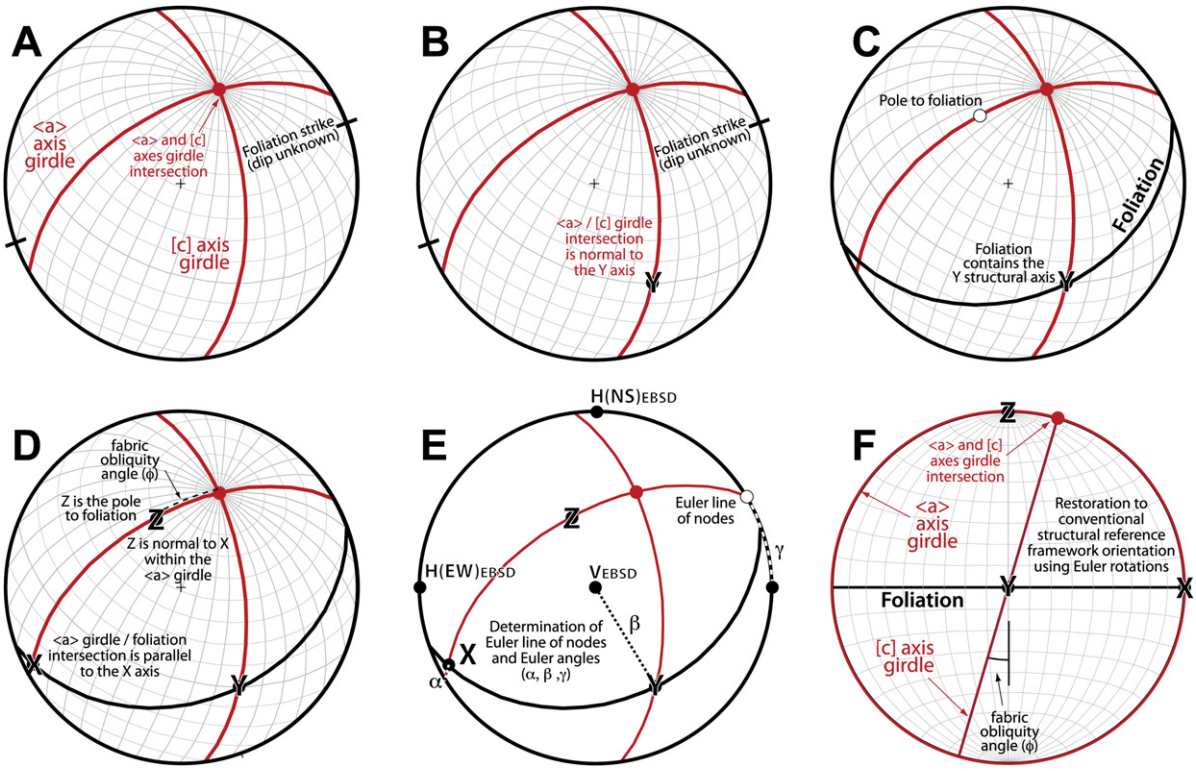


**Fig. 6.** Lower hemisphere stereographic projections explaining the procedure followed to rotate EBSD measured raw quartz LPOs. A: The quartz [c] and ⟨a⟩ LPOs measured in pebbles whose structural reference framework is unknown are used to identify major circles that fit best the girdle or point maxima distributions. B: The Y structural axis is located along the [c] axis girdle, 90° apart from the [c] and ⟨a⟩ girdle intersection. C: The location of Y and the strike of the foliation are used to reconstruct the orientation of the pebble foliation (XY structural plane) and its pole. D: The Z structural direction coincides with the pole to the foliation and the X direction is normal to both Y and Z. The misfit between Z and the [c] and ⟨a⟩ girdle intersection is the fabric obliquity angle. E: The referential for EBSD measurements and the XYZ structural reference are related through the Euler angles (see text for further details). F: Once the Euler angles are determined, the original quartz [c] and ⟨a⟩ crystallographic axis fabrics can be rotated so that X appears oriented horizontal East-West, Z horizontal normal to X, and Y vertical, as in conventional fabric diagrams.

axis, whereas β is the angle between the Y structural axis and the vertical EBSD referential and, finally, γ is the angle between the line of nodes and the horizontal E-W EBSD referential. The sign convention followed was the described by Ramsay and Huber (1983, p. 168). Various sets of Euler angles, each related to one of the quartz pebble fabrics measured, were used as inputs in the Channel5 software to recalculate and redraw the fabric stereoplots as conventional fabric diagrams (Fig. 6F). The results are presented and interpreted in the following section 4.

## 4. Quartz pebble syn-metamorphic fabrics

### 4.1. Microstructures and metamorphic grade

Microstructures and fabrics indicating syn-metamorphic ductile deformations can be recognized in several pebble sections. Foliations in polycrystalline quartz pebbles are defined by the parallel orientation of grain boundaries in combination with shape fabrics parallel or oblique to them (Fig. 3A, G, and H). In polymineralic aggregates (sandstones, quartzites and cherts) foliations are defined by the parallel orientation of graphite, mica and chlorite as well as by the elongation of quartz grains. These foliations are in some lithologies axial planar with microfolds showing slight limb thinning and hinge thickenning (Fig. 3H).

The mineral assemblages preserved in these pebbles denote very low-grade or low-temperature greenschists facies metamorphism. Polycrystalline quartz aggregates lack mineral assemblages appropriate to identify any metamorphic grade. However, they exhibit a considerable variety of microstructures resulting from ductile deformation (Fig. 7A–C, 8A-C and 9A-G). Microstructures pointing to dislocation creep (undulose extinction, deformation lamellae, subgrains with boundaries parallel to prism planes) and grain boundary migration (recrystallized new grains, shape fabrics, oriented mineral inclusions) are common. They characterize Hirth and Tullis' (1992) regime 1 of quartz plastic flow, which operates under temperatures below 250–300 °C and/or fast strain rates. Also present are microstructures denoting dislocation climb and recovery (subgrain formation, flattened grains), which characterize Hirth and Tullis' (1992) regime 2 of quartz plastic flow. These reflect deformation under higher temperature, slower strain rates and probably in the presence of a catalyzing fluid phase. Finally, mosaic microstructures and shape fabrics denote a complete dynamic recrystallization (through either subgrain rotation or grain boundary migration). The high mobility of grain boundaries is demonstrated here by the complete inclusion of oriented chlorite crystals by recrystallized quartz grains. These microstructures characterize Hirth and Tullis' (1992) regime 3 of quartz plastic flow, which occurs under higher temperatures (often above the transition between the greenschists and the amphibolite metamorphic facies) and slower strain rates than the regime 2.

### 4.2. High-temperature quartz fabrics

Some of the microstructures observed correspond to the "chessboard" microstructures of quartz (Bouchez et al., 1985), regarded as a microstructural geothermometer (Kruhl, 1996) that denotes plastic deformation under medium to high-grade

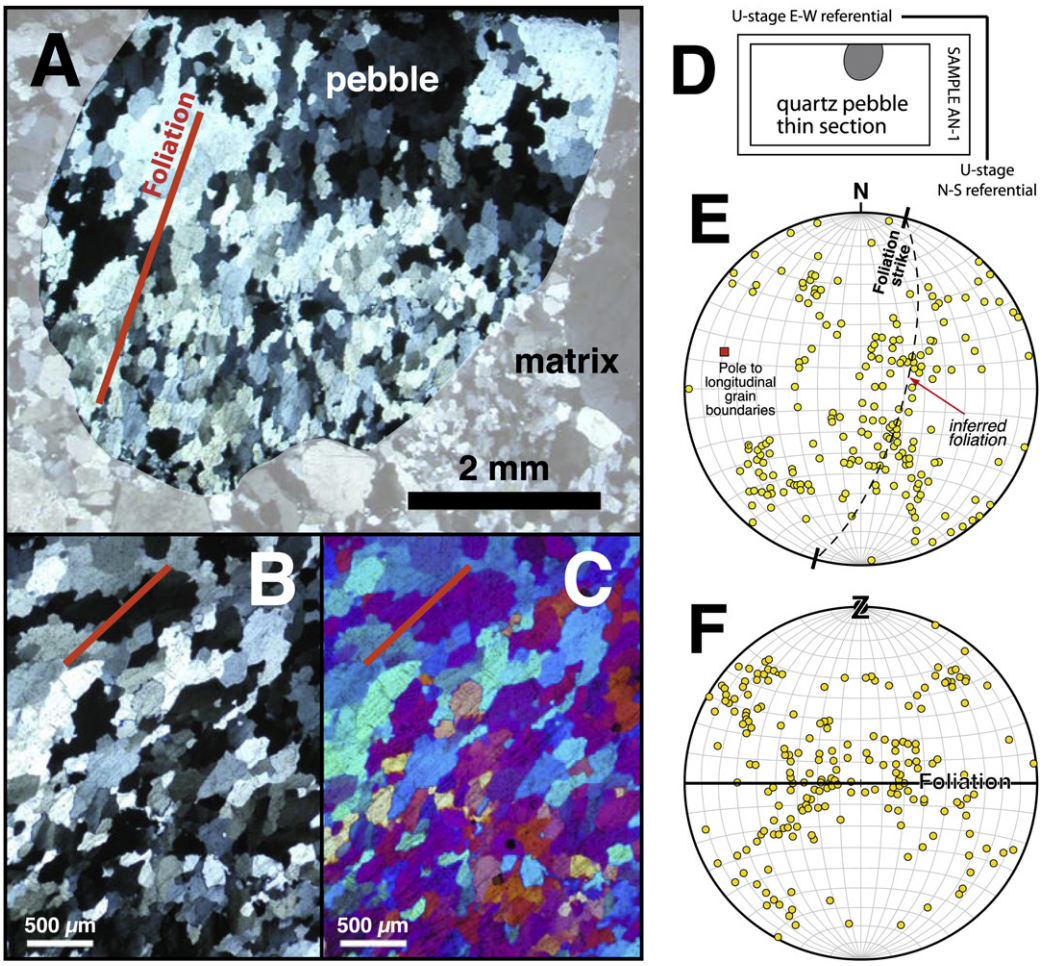


**Fig. 7.** A: Micrograph of a polycrystalline quartz pebble (crossed polars) with "chessboard" microstructure and a continuous foliation. B: Detail of A showing the statistical parallelism (or perpendicularity) between quartz grain boundaries and the foliation. C: Micrograph of the field of view B made with a compensation gypsum lens to highlight the preferred crystallographic orientation of the microstructure. D: Sketch of the conventional thin section that contains the pebble shown in A. E: Lower hemisphere, equal area stereographic projection of 200 quartz [c] axes measured from the thin section D and plotted taking its long and short edges as E-W and N-S referentials. F. Lower hemisphere, equal area stereographic projection of the 200 quartz [c] axes rotated so as to present the foliation vertical E-W. See text for further details.

metamorphic conditions and possibly under hydrous conditions and fast strain rates (Mainprice et al., 1985). They occur in pebbles with a prominent foliation and several quartz grains. When observed with crossed polars under the petrographic microscope, grains remain close to extinction while the stage is rotated 360°. This means that their [c] axes are normal to the plane of pebble sections, which thus are close to the orientation of the XZ structural plane. Chessboard subgrain and grain boundaries are parallel to prismatic and basal crystallographic planes (Tubía and Cuevas, 1985) due to prism-⟨a⟩ and prism-[c] intracrystalline slip in the high-quartz stability field (Kruhl, 1996). This highlights that ductile deformation was constrained by intracrystalline slip system transitions active at moderate to elevated temperature (above 550–600 °C under natural strain rates; Okudaira et al., 1995).

In the Figs. 7 and 8 we present the results of microfabric analysis and restoration of two polycrystalline quartz pebbles with the microstructure described above. Quartz grain shape fabrics are evident in both pebbles (Figs. 7A and 8A) and the chessboard arrangement of quartz grain boundaries is obvious in the Fig. 8A (and to a lesser extent in parts of the Fig. 7A). Petrographic observations with the gypsum plate permit to demonstrate that the quartz shape fabrics are related to crystallographic preferred orientations (Figs. 7B–C and 8B–C). The respective quartz [c] axis fabrics were determined with the U-stage, originally taking the thin section long and short edges (Figs. 7D and 8D) as horizontal E-W and N-S referentials. They are presented as raw stereoplots (with a sample reference frame) in the Figs. 7E and 8E, where the great circles represent foliation orientations determined after its strike in the thin sections and the mean tilt angle of grain boundaries parallel to that direction. Fabric rotations following the procedure described in section 3.3.1 resulted in the stereoplots presented in the Figs. 7F and 8F. In the Fig. 7F two perpendicular [c] axis girdles (the type II fabrics of Lister and Dornsiepen, 1982) intersect at a point close to the stereonet center and are oblique to the foliation and its pole. This pattern suggests that the structural X direction is close to a horizontal E-W line and that, thus, the stereonet horizontal plane actually coincides with the XZ structural section. It denotes activation of prism [c] slip in addition to the basal ⟨a⟩ and [c] intracrystalline slip systems. In the quartz pebble of Fig. 8 preservation of several grain boundaries perpendicular to the foliation enabled to determine the orientation of the X structural direction in addition to that of the foliation and its pole. This permitted to accomplish a complete rotation of the original fabric (Fig. 8E) to an XZ stereoplot (Fig. 8F). The most prominent feature of the restored fabric is a single [c] axis point maxima close to X and oblique to the XYZ framework. It denotes the high-temperature

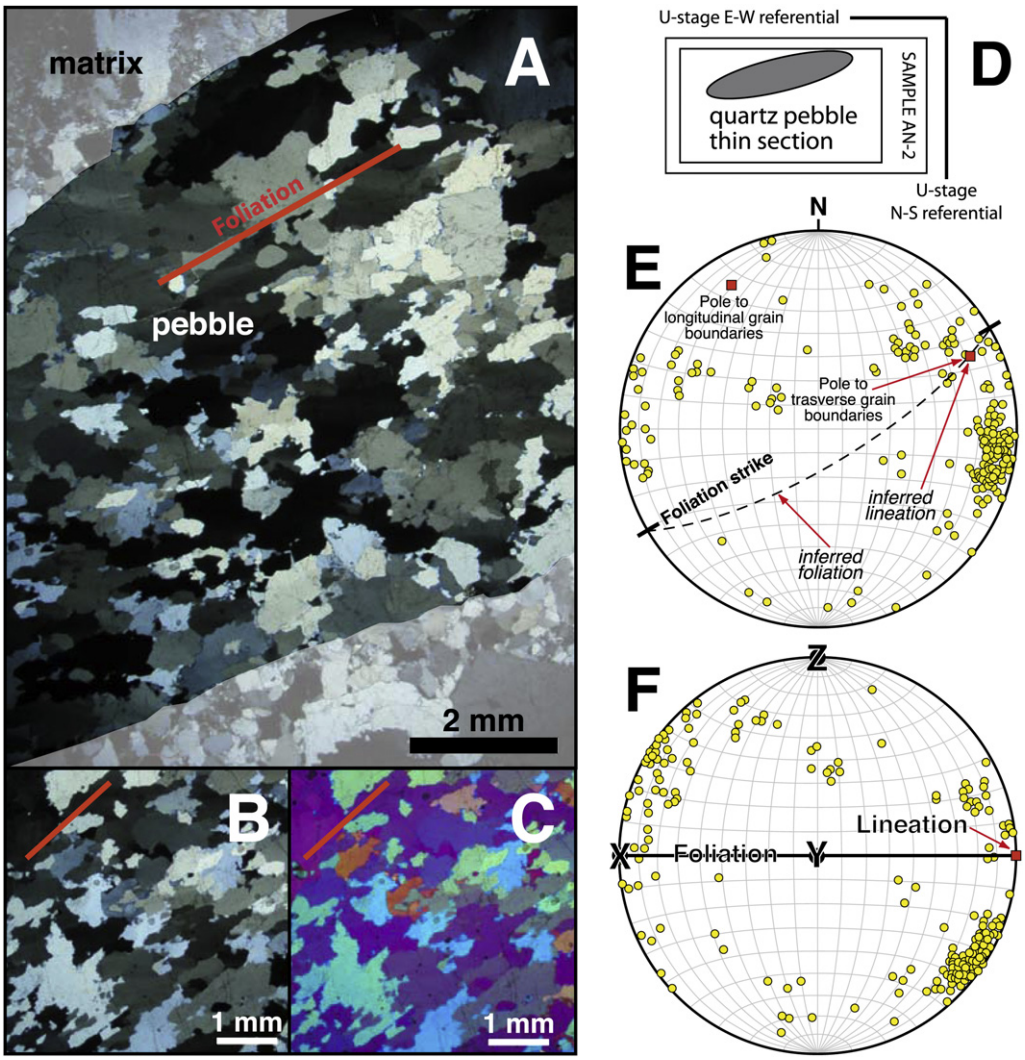


**Fig. 8.** See caption of Fig. 7. In F. the pebble foliation is vertical E-W and the quartz mineral lineation is horizontal within the foliation plane. See text for further details.

activation of prism [c] slip (at T of ca. 650 °C), as well as the non-coaxial character of ductile deformation.

The results of an EBSD-based study of subgrain and new grain misorientations associated to chessboard microstructures are presented in the Fig. 9. Micrographs 9A and 9C show two sample microstructures with the superposed tracks (running from the upper left to the lower right) of two straight lines along which quartz lattice orientations were recorded at steps of 10 μm. In the line graphs to the right (Fig. 9B and D) the misorientation angle of the quartz lattice at each track pixel (measured in °) with respect to the orientation of the adjoining one (the abscise refers to track distance in μm) is plotted. The misorientation angles correspond to rotations along specific, rationale crystallographic axes that can be labeled with the Channel5 software. The Fig. 9B line graph shows quartz grain boundaries that are systematically associated to 60° reorientations around the [0001] axis of the bounded lattices. Actually, these are quartz basal plane-parallel grain boundaries related to prism-[c] slip, hardly detectable with the petrographic microscope (Tubía and Cuevas, 1985). The 60° lattice rotation effect around the [0001] axis is likely due to Dauphiné twinning. Brazil twin planes, which are normal to quartz ⟨a⟩ axes, also separate right and left hand quartz lattices misoriented 60°, but are not detected by the EBSD technique. In order for Dauphiné twins to be produced by dislocations, they must be twist boundaries parallel with the basal plane. This requires dislocations slipping in the basal plane with more than one Burgers vector. Tullis and Tullis (1972) showed that Dauphiné twinning contributes to the total quartz fabric, as it may influence the relative activities of competing slip systems (Lister, 1979; Lister and Paterson, 1979). It operates independently of intracrystalline slip and does not reorient the [c] axis. The Fig. 9D line graph depicts misorientations below 1° (only a few times above 2°) along a large and non-uniform set of rationale directions for most parts of the track. In general, these can be considered orientation misfits below the measuring technique resolution and thus are disregardable.

### 4.3. Moderate- and low-temperature quartz deformation

The fabric of various pebbles made of polycrystalline quartz aggregates was studied with the EBSD technique (Fig. 10A–G). They exhibit a foliation and a dynamically recrystallized microstructure. The original crystallographic orientation data were measured at points regularly separated 10 μm and filtered before plotting them in the stereoplots. Channel5 software was used to discriminate between grains with misorientations above a critical threshold of 10°, allowing boundary completion down

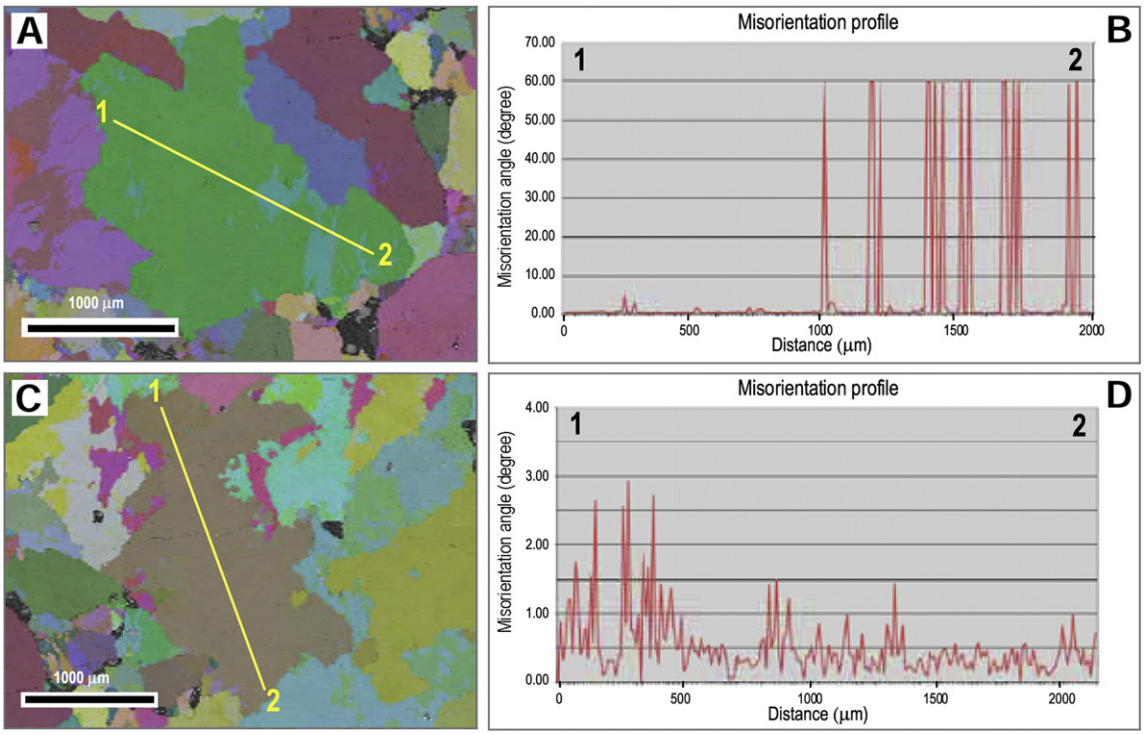


**Fig. 9.** A: EBSD orientation map of a "chessboard" quartz microstructure. Quartz crystallographic orientation along the transect 1–2 was recorded at steps of 10 μm. B: Plot of the quartz lattice misorientation angle between adjacent measurement points along the track 1–2 shown in A. C: Idem as A except that the misorientation profile is shown in D. D: Idem as B. See text for further details.

to 5°. A single crystallographic orientation was assigned to each grain and plotted in the stereograms. The fabrics obtained often show point and girdle axis distributions with general orientations with respect to the horizontal and vertical reference axes of the EBSD acquisition. The values of the texture index *J* vary between 1.18 and 4.46, thus characterizing moderate to intense fabrics.

In the Fig. 11 the quartz [c] and ⟨a⟩ LPOs are plotted in a horizontal XZ reference plane after the rotation procedure described in section 3.3.2 The monoclinic distribution of the [c] axes with respect to the XYZ framework is evident, denoting the non-coaxial character of quartz plastic deformation. The [c] axes appear arranged in point or girdle distributions. In the former case, they always contain point maxima concentrations along the Y axis, which are either isolated or combined with other concentrations close to Z or at positions between Y and Z. Except for the case of Fig. 11C, axis distributions correspond to incomplete girdles partly constrained by the three point maxima orientations already reported. Fabric asymmetry is not so straightforward from inspection of the ⟨a⟩ axes distributions. These are spread out along girdles close to the horizontal projection plane of the stereoplots that can contain point submaxima concentrations evenly spaced 60°. The features described can be interpreted as a result of the operation of the prism-⟨a⟩ intracrystalline slip system in all the fabrics, in addition to basal ⟨a⟩ slip in some cases (Fig. 11A–C) and rhomb-⟨a⟩ slip in others (Fig. 11D, E and G). This unravels quartz plastic deformation under moderate temperatures (Fig. 4) of the greenschists or low-T amphibolite metamorphic facies. The quartz fabric of Fig. 11E presents an incomplete [c] axis girdle forming a low angle with the foliation, thus resembling operation of prism-[c] slip under higher deformation temperatures. The distribution of the ⟨a⟩ axes along the periphery of the steroplot, however, precludes such an interpretation, since the pattern expected for prism-[c] slip is a girdle normal to the X direction (Fig. 4).

The monocrystalline quartz pebble group includes pebbles of variable size in which petrographic inspection enables to recognize that they are made either of a single quartz crystal or of a small number of crystals with a close orientation (subgrains). The second were studied with the EBSD technique (Fig. 12). The original crystallographic orientation data set was filtered with the Channel5 software before plotting in the stereographs by considering misorientations above 5–10° (as described above). The fabrics obtained contain a single [c] axis point maxima normal to ⟨a⟩ axis girdles made of three point maxima separated 60° among them. The strength of these fabrics is remarkable according to the texture index *J*, which attains values of up to 12.0. Low and high-angle grain boundaries are widespread and exhibit complex, sutured geometries. Distinction between old grains and recrystallized subgrains is not evident always. The variation of [c] or ⟨a⟩ axis orientations within each pebble attains 20° with respect to the orientation of the maximum density concentrations. This figure clearly exceeds the limit used to discriminate dynamically recrystallized new grains reported above, but should be interpreted taking into account that it does not relate to subgrains in direct contact misoriented up to 20° (which would imply they are new grains instead of subgrains) but to sets of subgrains (from the subgrain population of a given pebble) that were progressively and accumulatively misoriented relative to each other. These microfabric and textural features enable us to interpret that the monocrystalline quartz pebbles endured cold working under temperatures lower than those inferred for the plastic deformation of the polycrystalline pebbles.

Some quartz pebbles that resemble polycrystalline aggregates because they exhibit a foliation and a recrystallized microstructure produced crystallographic fabrics similar to those of the

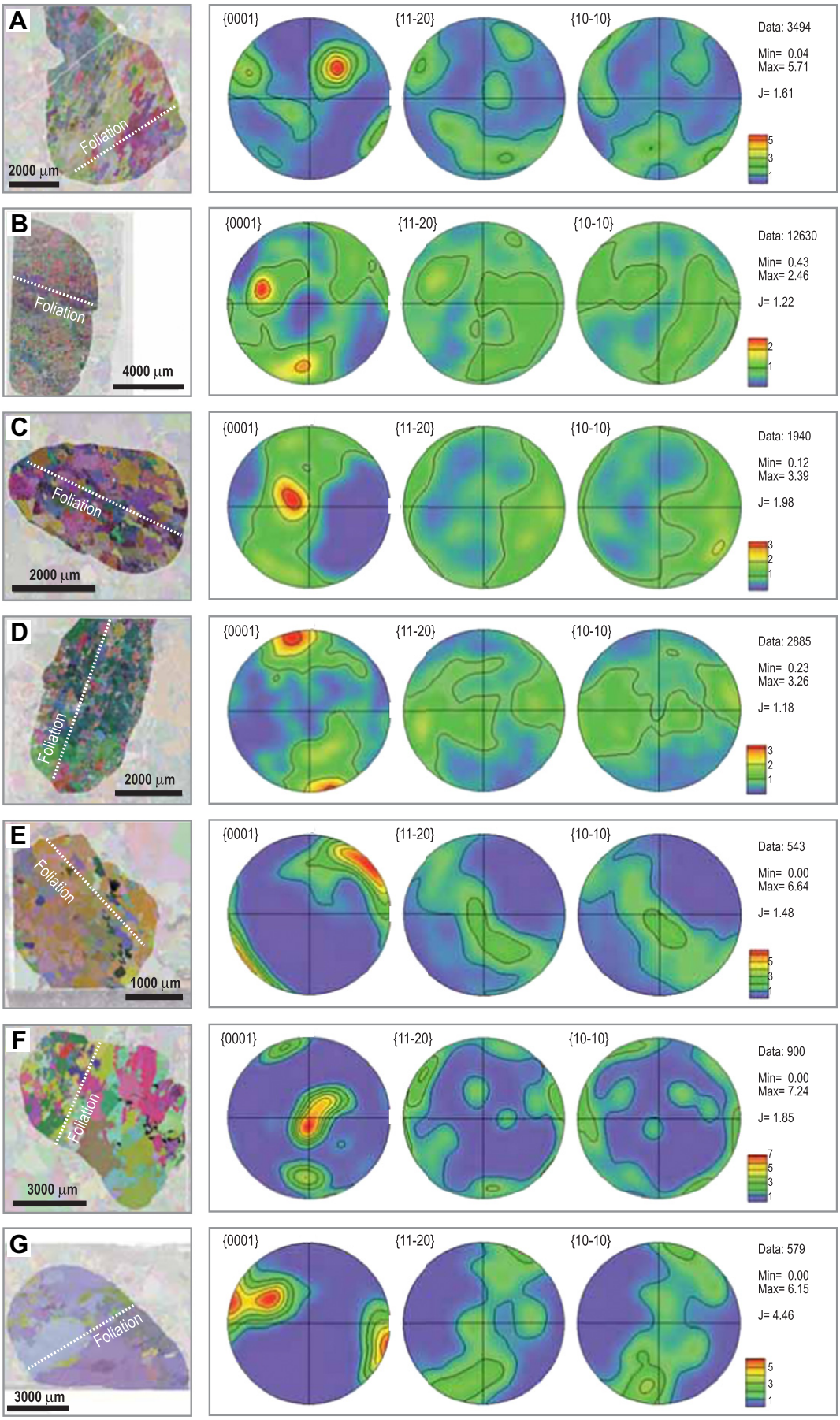
A
Foliation
2000 μm
{0001}
{11-20}
{10-10}
Data: 3494
Min= 0.04
Max= 5.71
J= 1.61
5
3
1
B
Foliation
4000 μm
{0001}
{11-20}
{10-10}
Data: 12630
Min= 0.43
Max= 2.46
J= 1.22
2
1
C
Foliation
2000 μm
{0001}
{11-20}
{10-10}
Data: 1940
Min= 0.12
Max= 3.39
J= 1.98
3
2
1
D
Foliation
2000 μm
{0001}
{11-20}
{10-10}
Data: 2885
Min= 0.23
Max= 3.26
J= 1.18
3
2
1
E
Foliation
1000 μm
{0001}
{11-20}
{10-10}
Data: 543
Min= 0.00
Max= 6.64
J= 1.48
5
3
1
F
Foliation
3000 μm
{0001}
{11-20}
{10-10}
Data: 900
Min= 0.00
Max= 7.24
J= 1.85
7
5
3
1
G
Foliation
3000 μm
{0001}
{11-20}
{10-10}
Data: 579
Min= 0.00
Max= 6.15
J= 4.46
5
3
1

monocrystalline quartz pebbles (Fig. 13). The texture index *J* of their LPOs, however, varies between 1.34 and 3.82. The fabrics contain single [c] axis point maxima normal to ⟨a⟩ axis girdles made of three ill defined point maxima separated 60°. The variation of the [c] or ⟨a⟩ axis orientations within each pebble usually exceeds the 20° reported in the precedent paragraph with respect to the orientation of the maximum density concentrations, and even reaches 30–40°. A more intense, protracted or hotter plastic deformation of former quartz monocrystals can be inferred for these pebbles, but interpretations on the active intracrystalline slip systems cannot be made with confidence after the data available.

### 4.4. Microchert pebbles and conglomerate matrix fabrics

Black chert pebbles exhibit petrographic evidence of either brittle or ductile deformation. The small size of quartz grains makes it impossible to ascertain from petrographic inspection if they underwent crystal plasticity or any other deformation mechanism (volume diffusion, solution-precipitation). Our EBSD study shows that microcherts lack any crystallographic preferred orientation (Fig. 14A and B), the texture index *J* being very low. This suggests that ductile deformation was assisted by mechanisms different from the crystal plasticity reported for quartz pebbles. However, it does not exclude a comparable tectonic setting (under low to moderate temperature conditions) prevalent during their folding and foliation development. Trepmann et al. (2010) have shown that dissolution-precipitation creep at low differential stress can be a deformation mechanism operative under low-grade metamorphic conditions (of up to 350 °C) promoting foliation development in quartzose rocks.

The matrix quartz aggregates (Fig. 14C) lack any crystallographic preferred orientation. The preservation of intact diagenetic microtextures and the lack of macroscopic or petrographic evidence of ductile strain suggests that the conglomerates behaved as mechanically brittle, competent units during most of their Paleozoic burial history after deposition and during subsequent Variscan and Alpine deformations.

## 5. Discussion

The Anguiano Conglomerate is an outstanding example of quartz-pebble conglomerate. This rock type is thought to represent tectonically quiescent conditions under which weathering (chemical and mechanical) was very efficient and included protracted transport, prolonged mechanical abrasion, intense chemical weathering or recycling of older conglomerate (Cox et al., 2002, and references therein). Its occurrence in the geological record increases backward through time, most examples being Proterozoic. Cox et al. (2002) suggested that this rock forms by postdepositional diagenetic alteration (clast disintegration/dissolution along pebble boundaries, porosity collapse by compaction and cementation) of polymict conglomerate precursors. Therefore, in spite of being made of more than 90% of quartz, chert or quartzite clasts, it is usually derived from lithological diverse sources (Grange et al., 2010). Petrographic evidence described in the section 2.2 of this study demonstrates quartz dissolution from pebbles and precipitation in the conglomerate matrix (as syntaxial overgrowths of sand-sized quartz grains and primary porosity fillings). The only evidence of a polymict conglomerate composition consists of accessory minerals such as tourmaline, zircon, rutile and scarce mica, as well as of the various quartzose pebble lithologies (metachert, sandstone, quartzite and vein quartz). Any other original pebble composition, had it really existed, would have been disintegrated by postdepositional diagenetic alteration.

The textural characteristics of the Anguiano Conglomerate pebbles and the relationships with their matrix/cement permit to interpret that they preserve microfabrics originally formed in the source rocks and that, thus, pebble quartz plastic deformation was acquired during stages of their tectonic history preceding erosion and early Cambrian deposition. Our petrographic, U-stage and EBSD fabric study, together with the fabric restoration method used, enabled us to identify deformations produced under temperatures characteristic of low-, medium- and high-grade metamorphism. The original tectonic setting was an orogenic environment that actually exposed in the pre-early Cambrian Earth's surface rocks that had been buried previously to variable depths. It also contained non-metamorphic silicic metasediments and a broad variety of recrystallized quartz veins, likely of igneous affinity. The occurrence of detrital zircon grains with internal magmatic microstructures in metasandstone pebbles and in the matrix point to the occurrence of magmatic precursors in the source areas. Detrital tourmaline is often common in those pebbles and the matrix, but this mineral might be related either to magmatic precursors or to metamorphic/hydrothermal recycling of preexisting tourmaline-bearing rocks, boron-rich sediments or even marine evaporites (Dini et al., 2008; Pérez-Xavier et al., 2008; Torres-Ruiz et al., 2003). Bea et al. (2009) have highlighted the potential of this mineral to date orogenic deformation phases. Rutile associated to zircon relics in foliated metasandstone pebbles point toward medium- to high-grade metamorphic or plutonic source rocks.

Andersen and Picard (1971) discussed how quartz pebble types had previously been used in provenance studies. This question, as well as those discussed above, bear on the characterization of currently concealed sediment provenance regions. Garzanti et al. (2007) distinguished five types of orogenic domains as the primary building blocks of composite orogens, each producing predictable detrital modes, heavy mineral assemblages and unroofing trends. Their "axial belt" (the metamorphic backbone of collisional orogens) and, to a lesser extent, "magmatic arc" source regions are the best candidates in our case study. According to Ugidos et al. (2010, and references therein), in the case of the Iberian realm these regions would correspond to reworked orogenic belts and internal cratons of peri-Gondwanan affinity whose remnants are preserved in Neoproterozoic to early Paleozoic sedimentary successions.

The lithological and accessory mineral evidence preserved in the Anguiano Conglomerate suggests that magmatic, low- to high-grade metamorphic and sedimentary rocks conformed the conglomerate source area. It might be reasonably expected that the outcrops of those source rocks would not occur too far from the current conglomerate outcrops. Source candidates include three tectonic settings: (1) the outcropping Neoproterozoic domains of the Iberian Massif (located toward the West), (2) the poorly known mid- and lower crustal segments of the Iberian microplate continental margin (Gardien et al., 2000), and (3) the concealed Ebro Massif (located toward the East), currently hindered under a km-thick Mesozoic to Tertiary cover.

**Fig. 10.** EBSD maps (labeled A-G, located to the left) and raw crystallographic fabrics of polycrystalline quartz pebbles. The surrounding matrix is displayed with a lighter color palette. Equal area, lower hemisphere stereographic projections with density color patterns and added contour lines in multiples of uniform distribution. "Min" and "Max" correspond to the minimum and maximum density concentration values. "J" is the texture index. Crystallographic notation: the poles of the family of planes {0001} are the quartz [c] axes, whereas the poles to the sets of planes {11-20} or {10-10} correspond to the ⟨a⟩ axes. See text for further details. (For interpretation of the references to color in this figure legend, the reader is referred to the web version of this article).

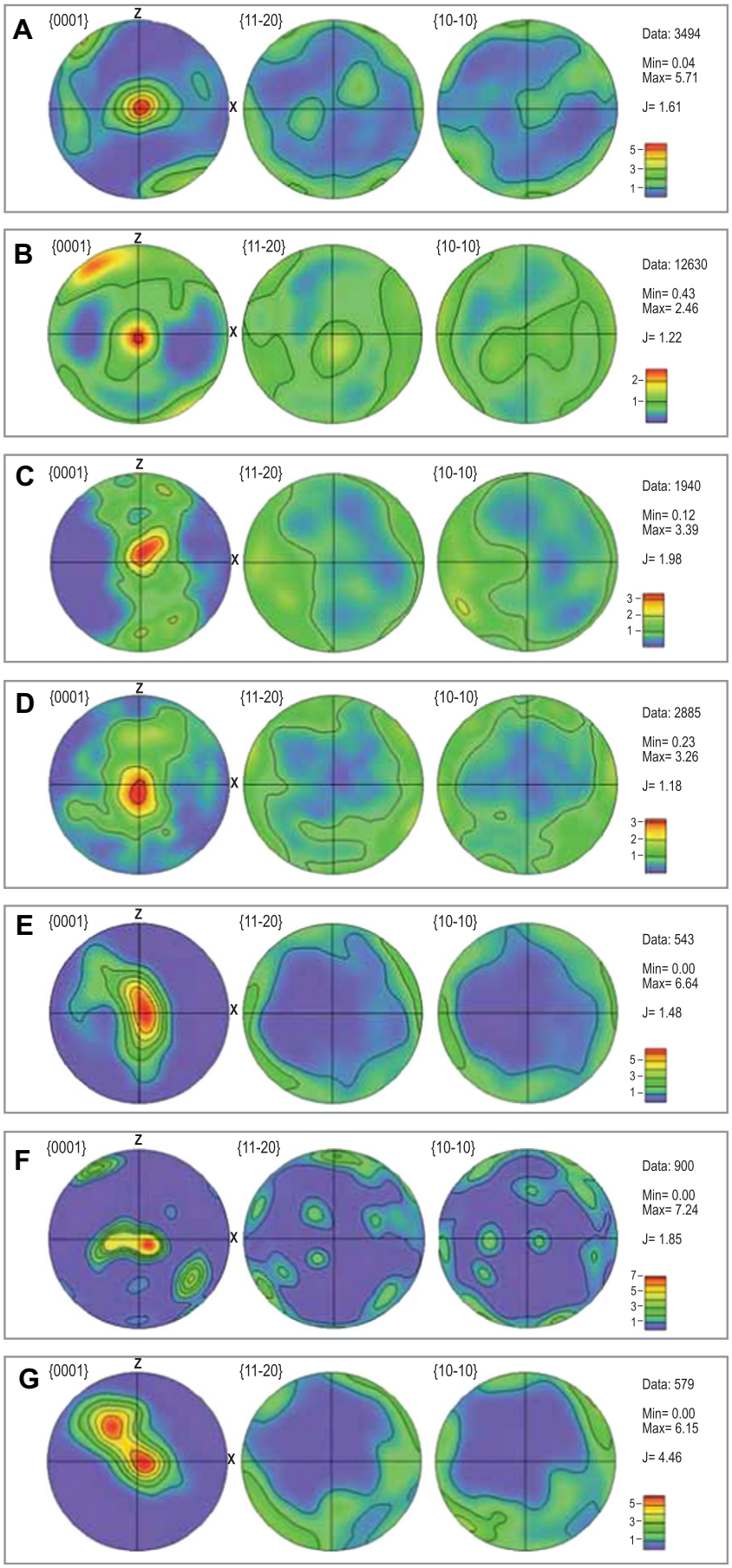


**Fig. 11.** Quartz LPOs for the polycrystalline quartz pebbles shown in the Fig. 10, plotted in a horizontal XZ reference plane after the rotation procedure described in the Fig. 6 and the manuscript. See caption to Fig. 10 and the text for further details.

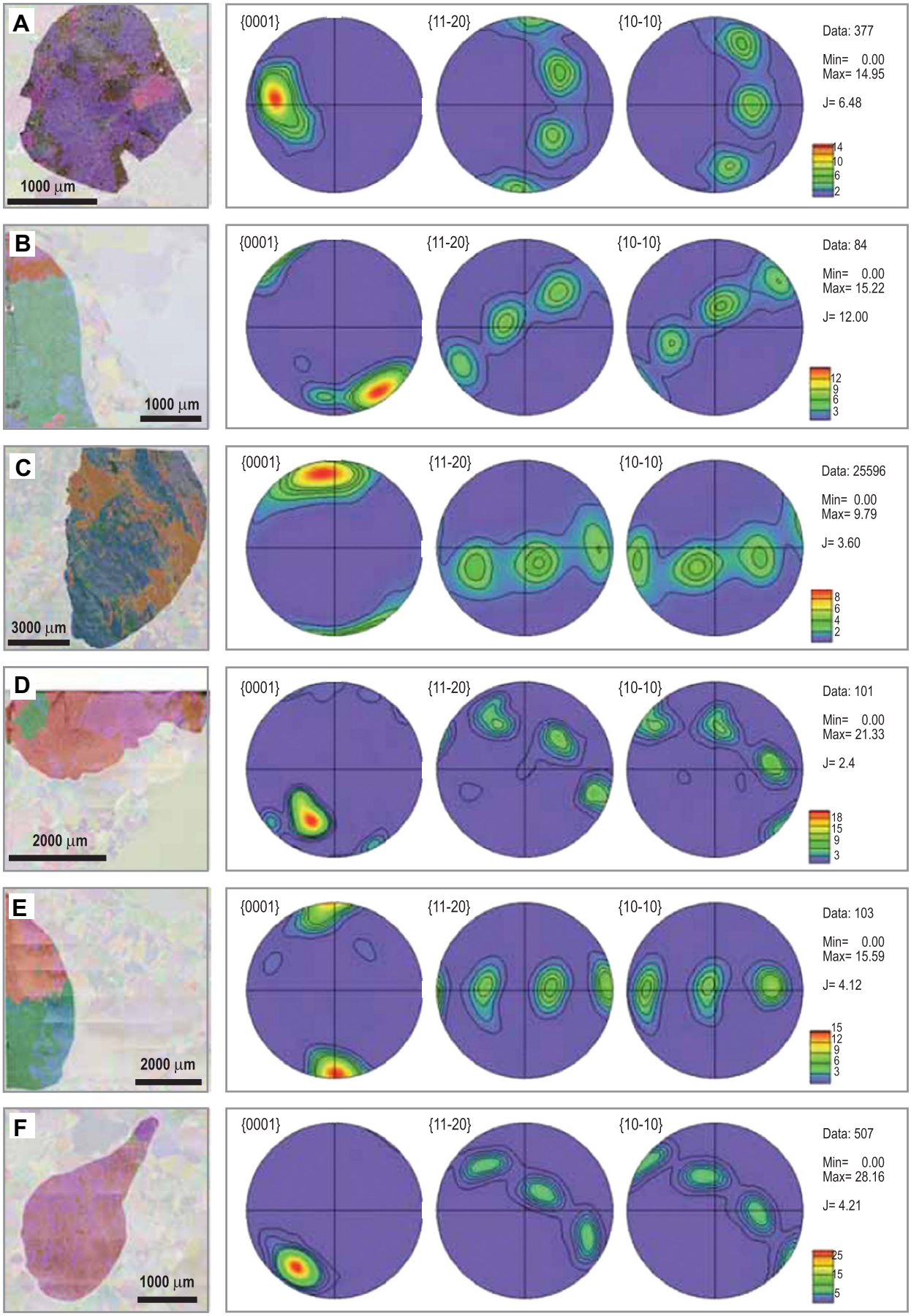


**Fig. 12.** EBSD maps (labeled A–F and located to the left of the figure) and raw crystallographic fabrics of various monocrystalline quartz pebbles. See caption to the Fig. 10 for further details.

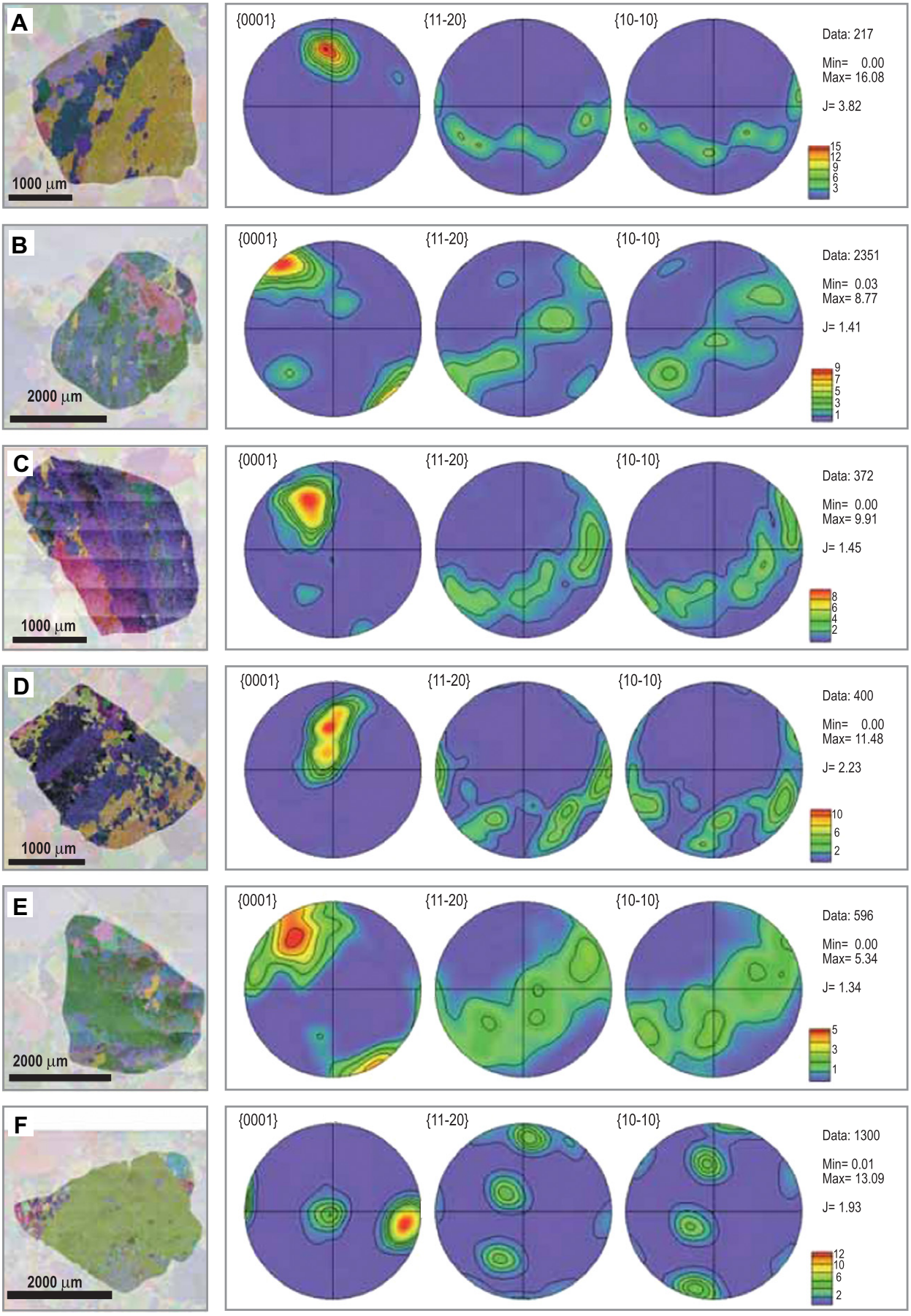


**Fig. 13.** EBSD maps (labeled A–F and located to the left of the figure) and raw crystallographic fabrics of various quartz pebbles apparently resembling polycrystalline aggregates. See caption to the Fig. 10 for further details.

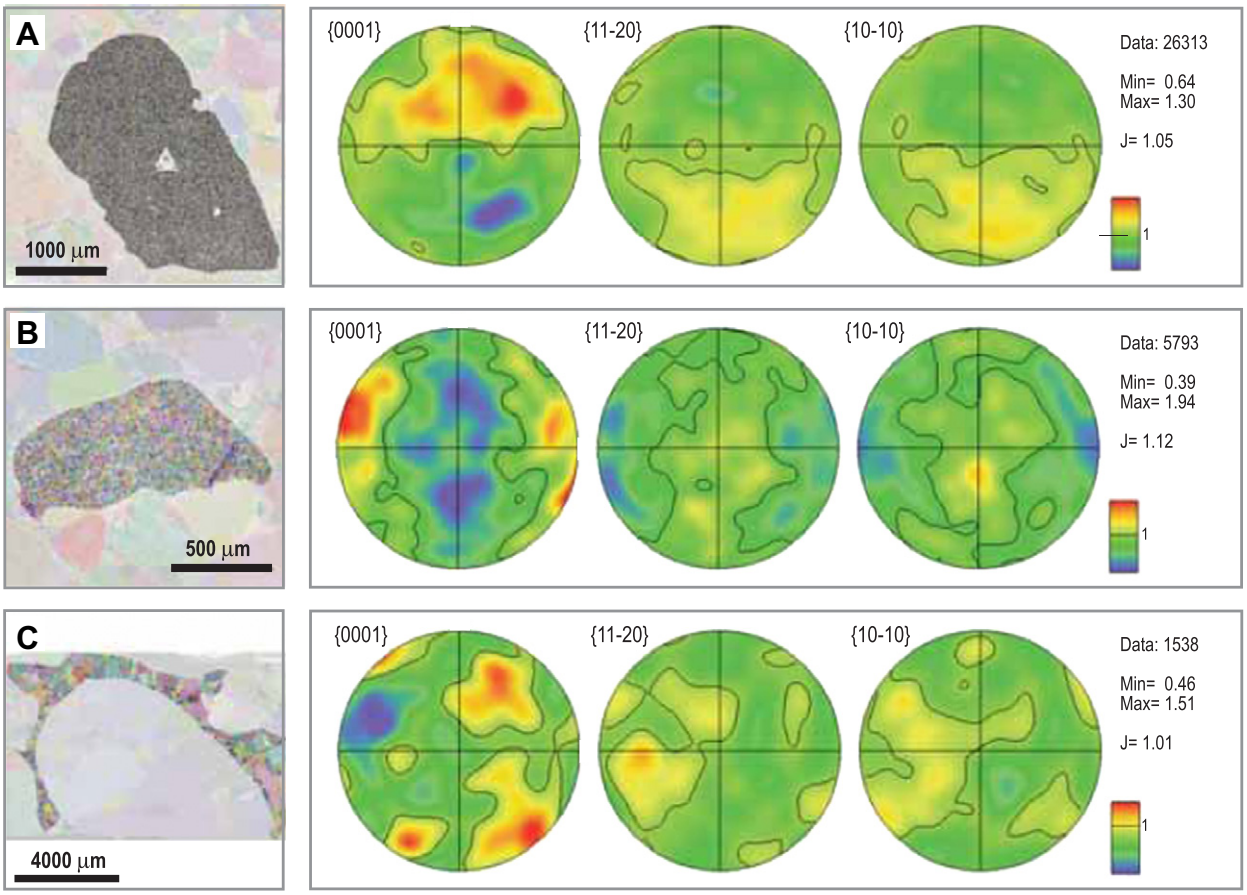


**Fig. 14.** EBSD maps (labeled A–C and located to the left of the figure) and raw crystallographic fabrics for black chert pebbles (A and B) and the quartzose matrix among pebbles (C). See caption to the Fig. 10 for further details.

As regards the first case, low- to high-grade, NeoProterozoic metamorphic rocks showing high-temperature ductile quartz deformation are only known to occur in the Ossa-Morena Zone (Ábalos, 1992; Ábalos and Eguíluz, 1992), a peri-Gondwanan magmatic arc accreted to the Iberian autochthon during the Cadomian orogeny (Ábalos et al., 2002 and references therein). These rocks exhibit a remarkable and widespread Neoproterozoic magmatic arc affinity that is not evident in the Sierra de la Demanda. Álvaro and Vennin (1998) reported the occurrence of schist pebbles (in addition to quartzite, metasediment and black quartzite ones) in early Cambrian conglomerates of the central Iberian Ranges. These constitute the Daroca Formation, which is slightly younger than the Anguiano Conglomerate. The authors interpreted that the source area of the pebbles contained igneous and metamorphic rocks also compatible with an "axial belt" or "magmatic arc" tectonic setting. As regards the second source candidate, so far it is known to exist in the thinned continental margins of the Bay of Biscay and the Galicia Bank (Gardien et al., 2000), though its autochthonous setting is unknown. Radiometric datings permitted to identify them as Neoarchean to Paleoproterozoic metamorphic rocks, some of which were already exhumed in the Mesoproterozoic. Finally, the geological constitution of the Ebro Massif remains largely unknown, as to our knowledge it has never been drilled and its existence is suggested by stratigraphic studies on the source regions of terrigenous Mesozoic successions outcropping in the Iberian Ranges and parts of the Basque Cantabrian Basin.

The wealth of radiometric ages recovered from inherited detrital zircon grains from different parts of the Iberian Massif have provided accurate time constraints on the source regions of the Neoproterozoic sedimentary rocks (Fernández-Suárez et al., 1999, 2000, 2002, 2003; Gutiérrez Alonso et al., 2005; Abati et al., 2010). These relate notably to Neoproterozoic (Pan-African and Cadomian) orogens, and to a lesser extent to Paleoproterozoic (1.8–2.1 Ga) or Neoarchean (2.4–2.8 Ga) ones, that resemble the West-African craton (e.g.: Ugidos et al., 1997; Valladares et al., 2002b). Mesoproterozoic relics were found in units of exotic origin (allochthonous) with respect to the Iberian Massif and in autochthon, Neoproterozoic to early Paleozoic sedimentary successions (e.g.: Fernández Suárez et al., 2003; Gutiérrez Alonso et al., 2005).

We argue that the source area of the Anguiano Conglomerate, with pebbles that preserve medium- to high-grade metamorphic fabrics, would correspond to current mid- to lower crustal settings of the Iberian microplate. These might either be related to the concealed Ebro Massif or to crustal segments buried under the Neoproterozoic successions of the Iberian Massif. The radiometric datings of high-grade metamorphic rocks recovered from the continental margins of the Bay of Biscay suggest that some of them (of Neoarchean to Paleoproterozoic age) were already exhumed in the Mesoproterozoic (Gardien et al., 2000). Neoproterozoic orogenic processes are better documented in the Iberian Peninsula and might have provided source metamorphic tectonite components for the Anguiano Conglomerate, too. Combined radiometric and metamorphic grade studies of recycled tectonite relics would be still more efficient to constrain provenance studies.

## 6. Conclusions

Conglomerate pebbles encapsulate structures and microfabrics that carry a memory of tectonic activity older than the age of the hosting sedimentary formations. Structural analysis of such pebble fabrics is precluded by the difficulty, or impossibility, to unravel any external structural reference framework to which refer petrographic observations or petrofabric measurements following the conventional procedures. The pebbles are sawed with a general, statistically unspecified orientation with respect to their internal foliation and lineation and, under this circumstance, microstructural observations are of limited value. Except in special cases, most crystallographic preferred orientation measurements would be difficult to interpret in terms of intracrystalline slip systems and deformation temperature or regime. These shortcomings can be resolved with the fabric rotation methods described in this study, applied to quartz LPO data acquired with the U-stage and the EBSD.

The quartz microstructures and the crystallographic fabrics presented in this article permit to constrain the kinematic framework of pre-early Cambrian tectonite pebbles and unravel the slip systems active during their ductile deformation. This gave us a way to identify deformations produced under temperatures characteristic of low-, medium- and high-grade metamorphism. Source rock candidates for the Anguiano conglomerate include Neoproterozoic units as those outcropping in the northern Iberian Massif, Neoproterozoic medium- to high-grade metamorphic rocks as those of SW Iberia, or a poorly known Neoarchean to Mesoproterozoic basement concealed under the Iberian Phanerozoic successions.

## Acknowledgments

The scientific comments of O. Fernandez, M. Pearce, G. Zulauf and an anonymous reviwer, and the editorial handling of J. Hippert, helped to improve the quality of the original manuscript and are sincerely acknowledged. Financial support was provided by the Spanish Ministerio de Ciencia e Innovación (Grupo Consolidado, project CGL2008-01130/BTE) and the Universidad del País Vasco (project GIU09/61).

## References

Ábalos, B., 1992. Variscan shear-zone deformation of late Precambrian basement in SW Iberia, implications for circum-Atlantic pre-Mesozoic tectonics. Journal of Structural Geology 14, 807–823. doi:10.1016/0191-8141(92)90042-U.

Ábalos, B., 2001. Nuevos datos microestructurales sobre la existencia de deformaciones precámbricas en la Sierra de la Demanda (Cordillera Ibérica). Geogaceta 30, 3–6.

Ábalos, B., Eguíluz, L., 1992. Structural geology of the Mina Afortunada Gneiss Dome (Badajoz-Córdoba shear zone, SW Spain). Annales Tectonicæ 6, 95–110.

Ábalos, B., Carreras, J., Druguet, E., Escuder Viruete, S., Gómez Pugnaire, M.T., Lorenzo Álvarez, S., Quesada, C., Rodríguez Fernández, L.R., Gil Ibarguchi, J.I., 2002. Variscan and pre-Variscan tectonics. In: Gibbons, W., Moreno, T. (Eds.), The Geology of Spain. Geological Society, London, pp. 156–183.

Abati, J., Gerdes, A., Fernández Suárez, J., Arenas, R., Whitehouse, M.J., Díez Fernández, R., 2010. Magmatism and early-Variscan continental subduction in the northern Gondwana margin recorded in zircons from the basal units of Galicia, NW Spain. Geological Society of America Bulletin 122, 219–235. doi:10.1130/B26572.1.

Álvaro, J.J., Vennin, E., 1998. Stratigraphic signature of a terminal Early Cambrian regressive event in the Iberian Peninsula. Canadian Journal of Earth Sciences 35, 402–411.

Álvaro, J.J., Bauluz, B., Gil-Imaz, A., Simón, J.L., 2008. Multidisciplinary constraints on the Cadomian compression and early Cambrian extension in the Iberian Chains, NE Spain. Tectonophysics 461, 215–227. doi:10.1016/j.tecto.2008.04.006.

Andersen, D.W., Picard, M.D., 1971. Quartz extinction in siltstone. Geological Society of America Bulletin 82, 181–186.

Bea, F., Pesquera, A., Montero, P., Torres-Ruiz, J., Gil Crespo, P.P., 2009. Tourmaline $^{40}Ar/^{39}Ar$ chronology of tourmaline-rich rocks from Central Iberia dates the main Variscan deformation phases. Geologica Acta 7, 399–412. doi:10.1344/104.000001446.

Bouchez, J.L., Lister, G.S., Nicolas, A., 1983. Fabric asymmetry and shear sense in movement zones. Geologische Rundschau 72, 401–419.

Bouchez, J.L., Tubía, J.M., Mainprice, D., 1985. Déformation naturelle du quartz: coexistence des systémes de glissement de direction -a- et -c- á haute temperature (migmatites de la nappe d'Ojén, Espagne). Comptes Rendus de l'Académie des Sciences de Paris 301, 841–846.

Bunge, H.J., 1985. Representation of preferred orientations. In: Wenk, H.-R. (Ed.), Preferred Orientation in Deformed Metals and Rocks: An Introduction to Modern Texture Analysis. Ed. Academic Press, Orlando, pp. 73–108.

Capote, R., Muñoz, J.A., Simón, J.L., Liesa, C.L., Arlegui, L.E., 2002. Alpine tectonics I: the Alpine system north of the Betic Cordillera. In: Gibbons, W., Moreno, T. (Eds.), The Geology of Spain. Geological Society, London, pp. 367–400.

Carls, P., 1983. La Zona Asturoccidental-Leonesa en Aragón y el macizo del Ebro como prolongación del Macizo Cantábrico. In: Comba, JA (Ed.), Contribuciones sobre temas generales. Libro Jubilar J.M. Ríos, v. 3. Instituto Geológico y Minero de España, Madrid, pp. 11–32.

Colchen, M., 1974. Géologie de la Sierra de la Demanda (Burgos-Logroño, Espagne). Memorias del Instituto Geológico y Minero de España 85, 1–436.

Cox, R., Gutman, E.D., Hines, P., 2002. Diagenetic origin for quartz-pebble conglomerates. Geology 30, 323–326.

de Sitter, L.U., 1961. Le Précambrien dans la Chaîne cantabrique. Comptes Rendus Sommaire des Séances de la Societé Géologique de France 9, 1–253.

Díaz García, F., 2006. Geometry and regional significance of Neoproterozoic (Cadomian) structures of the Narcea Antiform, NW Spain. Journal of the Geological Society, London 163, 499–508.

Dini, A., Mazzarini, F., Musumeci, G., Rocchi, S., 2008. Multiple hydro-fracturing by boron-rich fluids in the Late Miocene contact aureole of eastern Elba Island (Tuscany, Italy). Terra Nova 20, 318–326. doi:10.1111/j.1365-3121.2008.00823.x.

Fernández Suárez, J., Díaz García, F., Jeffries, T.E., Arenas, R., Abati, J., 2003. Constraints on the provenance of the uppermost allochthonous terrane of the NW Iberian Massif: inferences from detrital zircon U-Pb ages. Terra Nova 15, 138–144. doi:10.1046/j.1365-3121.2003.00479.X.

Fernández Suárez, J., Gutiérrez Alonso, G., Jeffries, T.E., 2002. The importance of along-margin terrane transport in northern Gondwana: insights from detrital zircon parentage in Neoproterozoic rocks from Iberia and Brittany. Earth and Planetary Science Letters 204, 75–88.

Fernández Suárez, J., Gutiérrez Alonso, G., Jenner, G.A., Jackson, S., 1998. Geochronology and geochemistry of the Pola de Allande granitoids (northern Spain). Their bearing on the Cadomian/Avalonian evolution of NW Iberia. Canadian Journal of Earth Sciences 35, 1–15.

Fernández Suárez, J., Gutiérrez Alonso, G., Jenner, G.A., Tubrett, M.N., 1999. Crustal sources in lower Paleozoic rocks from NW Iberia: insights from laser ablation U-Pb ages of detrital zircons. Journal of the Geological Society, London 156, 1065–1068.

Fernández Suárez, J., Gutiérrez Alonso, G., Jenner, G.A., Tubrett, M.N., 2000. New ideas on the Proterozoic-Early Paleozoic evolution of NW Iberia: insights from U-Pb detrital zircon ages. Precambrian Research 102, 185–206.

Gardien, V., Arnaud, N., Desmurs, L., 2000. Petrology and Ar-Ar dating of granulites from the Galicia Bank (Spain): African craton relics in Western Europe. Geodinamica Acta 13, 103–117.

Garzanti, E., Doglioni, C., Vezzoli, G., Andó, S., 2007. Orogenic belts and orogenic sediment provenance. Journal of Geology 115, 315–334.

Gil Imaz, A., 2001. La estructura de la Sierra de Cameros: deformación dúctil y su significado a escala cortical. Instituto de Estudios Riojanos, Logroño. Ciencias de la Tierra, 23, 1–305 (Ph.D. Thesis, Univ. Zaragoza, 1999).

Gozalo, R., Liñán, E., 1988. Los materiales hercínicos de la Cordillera Ibérica en el contexto del Macizo Ibérico. Estudios Geológicos 44, 399–404.

Grange, M.L., Wilde, S.A., Nemchin, A.A., Pidgeon, R.T., 2010. Proterozoic events recorded in quartzite cobbles at Jack Hills, Western Australia: new constraints on sedimentation and source of $>$ 4 Ga zircons. Earth and Planetary Science Letters 292, 158–169. doi:10.1016/j.epsl.2010.01.031.

Gutiérrez Alonso, G., Fernández Suárez, J., Collins, A.S., Abad, I., Nieto, F., 2005. Amazonian Mesoproterozoic basement in the core of the Ibero-Armorican Arc: 40Ar/39Ar detrital mica ages complement the zircons tale. Geology 33, 637–640. doi:10.1130/G21485.1.

Hatcher Jr., R.D., 1995. Structural Geology, Principles, Concepts and Problems, second ed. Prentice-Hall, Upper Saddle River, New Jersey, p. 525.

Hirth, G., Tullis, J., 1992. Dislocation creep regimes in quartz aggregates. Journal of Structural Geology 14, 145–159.

Julivert, M., Martínez García, E., 1967. Sobre el contacto entre el Precámbrico y el Cámbrico en la parte meridional de la cordillera Cantábrica y el papel del Precámbrico en la orogénesis Herciniana. Acta Geológica Hispánica 2, 107–110.

Kruhl, J.H., 1996. Prism- and basal-plane parallel subgrain boundaries in quartz: a microstructural geothermobarometer. Journal of Metamorphic Geology 14, 581–589.

Liesa, C.L., Casas Sainz, A.M., 1994. Reactivación alpina de pliegues y fallas del zócalo hercínico de la Cordillera Ibérica: ejemplos de la Sierra de la Demanda y la Serranía de Cuenca. Cuadernos del Laboratorio Geológico de Laxe 19, 119–135.

Liñán, E., Tejero, R., 1988. Las formaciones precámbricas del antiforme de Paracuellos (Cadenas Ibéricas). Boletín de la Real Sociedad Española de Historia Natural 84, 39–49.

Liñán, E., Perejón, A., Sdzuy, K., 1993. The lower–middle Cambrian stages and stratotypes from the Iberian Peninsula: a revision. Geological Magazine 130, 817–833.

Liñán, E., Gozalo, R., Palacios, T., Gámed-Vintaned, J.A., Ugidos, J.M., Mayoral, E., 2002. Cambrian. In: Gibbons, W., Moreno, T. (Eds.), The Geology of Spain. Geological Society, London, pp. 17–29.

Lister, G.S., 1979. Fabric transitions in plastically deformed quartzites: competition between basal, prism and rhomb systems. Bulletin de Minéralogie 102, 232–241.
Lister, G.S., Dornsiepen, U.F., 1982. Fabric transitions in the Saxony granulite terrain. Journal of Structural Geology 4, 81–92.
Lister, G.S., Paterson, M.S., 1979. The simulation of fabric development during plastic deformation and its application to quartzite: fabric transitions. Journal of Structural Geology 1, 99–115.
Lotze, F., 1957. Zum Alter nordwestpanischer Quartzit-Sandstein-Folgen. Neues Jahrbuch für Geologie und Paläontologie Monatshefte 10, 128–139.
Lotze, F., 1961. Das Kambrium Spaniens. Teil I: Stratigraphie. Abhandlungen der Gesellschaft der Wissenschaften zu Göttingen (Mathematisch-Physikalische Klasse) 6, 283–501.
Mainprice, D., Bouchez, J.L., Blumefield, P., Tubía, J.M., 1985. Dominat c-slip in naturally deformed quartz: implications for dramatic plastic softening at high temperature. Geology 14, 819–822.
Marcos, A., 1973. Las series del Paleozoico inferior y la estructura Herciniana del occidente de Asturias (NO de España). Trabajos de Geología 6, 1–113.
Martínez Catalán, J.R. 1985. Estratigrafía y estructura del Domo de Lugo (sector Oeste de la Zona Asturoccidental-Leonesa). Corpus Geologicum Gallaeciae 2, 1–291 (Ph.D. Thesis Univ. Salamanca, 1981).
Matte, Ph, 1967. Le Précambrien supérieur schisto-gréseux de l'Ouest des Asturies (Nord-Est de l'Espagne) et ses relations avec les séries précambriennes plus internes de l'arc galicien. Comptes Rendus de l'Académie des Sciences de Paris 264, 1769–1772.
Means, W.D., Hobbs, B.E., Lister, G., Williams, P.F., 1980. Vorticity and non-coaxiality in progressive deformations. Journal of Structural Geology 2, 371–378.
Okudaira, T., Takeshita, T., Hara, I., Ando, J., 1995. A new estimate of the conditions for transition from basal ⟨a⟩ to prism [c] slip in naturally deformed quartz. Tectonophysics 250, 31–46.
Palacios, T., 1982. El Cámbrico entre Viniegra de Abajo y Mansilla (Sierra de la Demanda, Logroño). Trilobites e ichnofósiles. Publicaciones del Instituto de Estudios Riojanos, pp. 1–86.
Palacios, T., Vidal, G., 1992. Lower Cambrian acritarchs from northern Spain: the Precambrian-Cambrian boundary and biostratigraphic implications. Geological Magazine 129, 421–436.
Passchier, C.W., Trouw, R.A.J., 1996. Microtectonics. Springer, Berlin-Heidelberg. p. 289.
Pérez Estaún, A., 1973. Datos sobre la sucesión estratigráfica del Precámbrico y la estructura del extremo Sur del Antiforme del Narcea (NW de España). Breviora Geologica Asturica 17, 5–16.
Pérez-Xavier, R., Wiedenbeck, M., Trumbull, R.B., Dreher, A.M., Monteiro, L.V.S., Rhede, D., de Araujo, C.E.G., Torresi, I., 2008. Tourmaline B-isotopes fingerprint marine evaporites as the source of high-salinity ore fluids in iron oxide copper-gold deposits, Carajás Mineral Province (Brazil). Geology 36, 743–746. doi:10.1130/G24841A.1.
Price, G.P., 1985. Preferred orientations in quartzite. In: Wenk, H.-R. (Ed.), Preferred Orientation in Deformed Metals and Rocks: An Introduction to Modern Texture Analysis. Ed. Academic Press, Orlando, pp. 385–406.
Prior, D.J., Boyle, A.P., Brenker, F., Cheadle, M.C., Day, A., Lopez, G., Potts, G.J., Reddy, S., Spiess, R., Timms, N., Trimby, P., Wheeler, J., Zetterstrom, L., 1999. The application of electron backscatter diffraction and orientation contrast imaging in the SEM to textural problems in rocks. American Mineralogist 84, 1741–1759.
Ramírez Merino, J.I., Olivé Davó, A., Álvaro López, M., Hernández Samaniego, A., 1990. Mapa y Memoria de la Hoja n° 241 (Anguiano) del Mapa Geológico de España a escala 1:50.000 (Serie MAGNA). Instituto Geológico y Minero de España, Madrid.
Ramsay, J.G., Huber, M.I., 1983. Strain Analysis. In: The Techniques of Modern Structural Geology, vol 1. Academic Press, London, pp. 1–307.
Schmid, S.M., Casey, M., 1986. Complete fabric analysis of some commonly observed quartz C-axis patterns. In: Mineral and Rock Deformation: Laboratory Studies. The Paterson Volume, vol 36. American Geophysical Union, Geophysical Monograph, pp. 263–286.
Schmidt-Thomé, M., 1973. Beiträge zur Feinstratigraphie des Unterkambriums in den Iberischen Ketten (Nordöst-Spanien). Geologisches Jahrbuch, Reihe B7, 3–43.
Schriel, W., 1930. Die Sierra de la Demanda und die Montes Obarenes. Abhandlungen der Gesellschaft der Wissenschaften zu Göttingen (Mathematisch-Physikalische Klasse). Neue Folge 16, 463–567.
Shergold, J.H., Liñán, E., Palacios, T., 1983. Late Cambrian trilobites from the Najerilla formation, north-eastern Spain. Palaeontology 26, 71–92.
Torres-Ruiz, J., Pesquera, A., Gil-Crespo, P.P., Velilla, N., 2003. Origin and petrogenetic implications of tourmaline-rich rocks in the Sierra Nevada (Betic Cordillera, southeastern Spain). Chemical Geology 197, 55–86.
Trepmann, C.A., Lenze, A., Stöckhert, B., 2010. Static recrystallization of vein quartz pebbles in a high-pressure – low-temperature metamorphic conglomerate. Journal of Structural Geology 32, 202–215. doi:10.1016/j.jsg.2009.11.005.
Trimby, P.W., Prior, D.J., Wheeler, J., 1998. Grain boundary hierarchy development in a quartz mylonite. Journal of Structural Geology 20, 917–935.
Tubía, J.M., Cuevas, J., 1985. Fábrica del cuarzo en tectonitas de alta temperatura (Manto de Ojén, Cordilleras Béticas). Estudios Geológicos 41, 147–155.
Tullis, J., Tullis, T.E., 1972. Preferred orientation produced by mechanical Dauphiné twinning: thermodynamics and axial experiments. American Geophysical Union. Monograph 16, 67–82.
Ugidos, J.M., Sánchez-Santos, J.M., Barba, P., Valladares, M.I., 2010. Upper Neoproterozoic series in the Central Iberian, Cantabrian and West Asturian Leonese Zones (Spain): geochemical data and statistical results as evidence for a shared homogenised source area. Precambrian Research 178, 51–58. doi:10.1016/j.precamres.2010.01.009.
Ugidos, J.M., Armenteros, I., Barba, P., Valladares, M.I., Colmenero, J.R., 1997. Geochemistry and petrology of recycled orogen-derived sediments: a case study from Upper Precambrian siliciclastic rocks of the Central Iberian Zone, Iberian Massif, Spain. Precambrian Research 84, 163–180.
Valladares, M.I., Barba, P., Ugidos, J.M., 2002a. Precambrian. In: Gibbons, W., Moreno, T. (Eds.), The Geology of Spain. Geological Society, London, pp. 7–16.
Valladares, M.I., Ugidos, J.M., Barba, P., Colmenero, J.R., 2002b. Contrasting geochemical features of the Central Iberian Zone shales (Iberian Massif, Spain): implications for the evolution of Neoproterozoic-lower Cambrian sediments and their sources in other peri-Gondwanan areas. Tectonophysics 352, 121–132.
Van Hise, C.R., Leith, C.K., 1909. Pre-Cambrian Geology of North America. United States Geological Survey Bulletin n° 360. Government Printing Office, Washington, pp. 1–939.
Vidal, G., Palacios, T., Gámez Vintaned, J.A., Díez Balda, M.A., Grant, S.W.F., 1994. Neoproterozoic-early Cambrian geology and palaeontology of Iberia. Geological Magazine 131, 729–765.